

- 6) Zheng X, Chung D, Takayama TK, Majerus EM, Sadler JE, Fujikawa K. Structure of von Willebrand factor-cleaving protease (ADAMTS13), a metalloprotease involved in thrombotic thrombocytopenic purpura. *J Biol Chem.* 2001; **276**: 41059-41063.
- 7) Levy GG, Nichols WC, Lian EC, et al. Mutations in a member of the ADAMTS gene family cause thrombotic thrombocytopenic purpura. *Nature.* 2001; **413**: 488-494.
- 8) Soejima K, Mimura N, Hirashima M, et al. A novel human metalloprotease synthesized in the liver and secreted into the blood: possibly, the von Willebrand factor-cleaving protease? *J Biochem.* 2001; **130**: 475-480.
- 9) von Willebrand EA. Hereditär pseudohemofili. *Finn Läkarsällsk Handl.* 1926; **67**: 7-112.
- 10) Nilsson IM, Blombäck M, Jörpes E, Blombäck B, Johansson SA. V. Willebrand's disease and its correction with human plasma fraction I-0. *Acta Med Scand.* 1957; **159**: 179-188.
- 11) Pool JG, Shanon AE. Production of high-potency concentrates of antihemophilic globulin in a closed-bag system. *N Engl J Med.* 1965; **273**: 1443-1447.
- 12) van Mourik JA, Mochtar IA. Purification of antihemophilic factor (factor VIII) by gel chromatography. *Biochim Biophys Acta.* 1970; **221**: 677-679.
- 13) Zimmerman TS, Ratnoff OD, Powell AE. Immunologic differentiation of classic hemophilia (factor VIII deficiency) and von Willebrand's disease: with observations on combined deficiencies of antihemophilic factor and proaccelerin (factor V) and on an acquired circulating anticoagulant against antihemophilic factor. *J Clin Invest.* 1971; **50**: 244-254.
- 14) Bouma BN, Wiegerinck Y, Sixma JJ, van Mourik JA, Mochtar IA. Immunologic characterization of purified antihemophilic factor A (factor VIII) which corrects abnormal platelet retention in Von Willebrand's disease. *Nat New Biol.* 1972; **236**: 104-106.
- 15) Toole JJ, Knopf JL, Wozney JM, et al. Molecular cloning of cDNA encoding human antihemophilic factor. *Nature.* 1984; **312**: 342-347.
- 16) Vehar GA, Keyt B, Eaton D, et al. Structure of human factor VIII. *Nature.* 1984; **312**: 337-342.
- 17) Sadler JE, Shelton-Inloes BB, Sorace JM, Harlan JM, Titani K, Davie EW. Cloning and characterization of two cDNAs coding for human von Willebrand factor. *Proc Natl Acad Sci USA.* 1985; **82**: 6394-6398.
- 18) Verweij CL, Diergaarde PJ, Hart M, Pannenkoek H. Full-length von Willebrand factor (vWF) cDNA encodes a highly repetitive protein considerably larger than the mature vWF subunit. *EMBO J.* 1986; **5**: 1839-1847.
- 19) Ginsberg D, Handin RI, Bonthron DT, et al. Human von Willebrand factor (vWF): Isolation of complementary DNA (cDNA) clones and chromosomal localization. *Science.* 1985; **228**: 1401-1406.
- 20) Shelton-Inloes BB, Titani K, Sadler JE. cDNA sequences for human von Willebrand factor reveal five types of repeated domains and five possible protein sequence polymorphisms. *Biochemistry.* 1986; **25**: 3164-3171.
- 21) van Mourik JA, Bouma BN, LaBruyère WT, De Graaf S, Mochtar IA. Factor VIII, a series of homologous oligomers and a complex of two proteins. *Thromb Res.* 1974; **4**: 155-164.
- 22) Ruggeri ZM, Zimmerman TS. Variant von Willebrand's disease: characterization of two subtypes by analysis of multimeric composition of factor VIII/von Willebrand factor in plasma and platelets. *J Clin Invest.* 1980; **65**: 1318-1325.
- 23) Berkowitz SD, Dent J, Roberts J, et al. Epitope mapping of the von Willebrand factor subunit distinguishes fragments present in normal and type IIA von Willebrand disease from those generated by plasmin. *J Clin Invest.* 1987; **79**: 524-531.
- 24) Dent JA, Berkowitz SD, Ware J, Kasper CK, Ruggeri ZM. Identification of a cleavage site directing the immunochemical detection of molecular abnormalities in type IIA von Willebrand factor. *Proc Natl Acad Sci USA.* 1990; **87**: 6306-6310.
- 25) Furlan M, Robles R, Lämmle B. Partial purification and characterization of protease from human plasma cleaving von Willebrand factor to fragments produced by *in vivo* proteolysis. *Blood.* 1996; **87**: 4223-4234.
- 26) Tsai HM. Physiologic cleavage of von Willebrand factor by a plasma protease is dependent on its conformation and requires calcium ion. *Blood.* 1996; **87**: 4235-4244.
- 27) Böhm M, Vigh T, Scharrer I. Evaluation and clinical application of a new method for measuring activity of von Willebrand factor-cleaving metalloprotease (ADAMTS13). *Ann Hematol.* 2002; **81**: 430-435.
- 28) Gerritsen HE, Turecek PL, Schwarz HP, Lämmle B, Furlan M. Assay of von Willebrand factor (vWF)-cleaving protease based on decreased collagen binding affinity of degraded vWF: a tool for the diagnosis of thrombotic thrombocytopenic purpura (TTP). *Thromb Haemost.* 1999; **82**: 1386-1389.
- 29) Furlan M, Robles R, Galbuseram M, et al. von Willebrand factor-cleaving protease in thrombotic thrombocytopenic purpura and the hemolytic-uremic syndrome. *N Engl J Med.* 1998; **339**: 1578-1584.
- 30) Tsai HM, Lian EC. Antibodies to von Willebrand factor-cleaving protease in acute thrombotic thrombocytopenic purpura. *N Engl J Med.* 1998; **339**: 1585-1594.
- 31) Cruz MA, Whitelock J, Dong JF. Evaluation of ADAMTS-13 activity in plasma using recombinant von Willebrand Factor A2 domain polypeptide as substrate. *Thromb Haemost.* 2003; **90**: 1204-1209.
- 32) Kokame K, Matsumoto M, Fujimura Y, Miyata T. VWF73, a region from D1596 to R1668 of von Willebrand factor, provides a minimal substrate for ADAMTS-13. *Blood.* 2004; **103**: 607-612.
- 33) Kokame K, Nobe Y, Kokubo Y, Okayama A, Miyata T. FRET-S-VWF73, a first fluorogenic substrate for ADAMTS13

- assay. *Br J Haematol.* 2005; **129**: 93-100.
- 34) Muia J, Gao W, Haberichter SL, Dolatshahi L, Zhu J, Westfield LA, Covill SC, Friedman KD, Sadler JE. An optimized fluorogenic ADAMTS13 assay with increased sensitivity for the investigation of patients with thrombotic thrombocytopenic purpura. *J Thromb Haemost.* 2013; **11**: 1511-1518.
- 35) Kato S, Matsumoto M, Matsuyama T, Isonishi A, Hiura H, Fujimura Y. Novel monoclonal antibody-based enzyme immunoassay for determining plasma levels of ADAMTS13 activity. *Transfusion.* 2006; **46**: 1444-1452.
- 36) Jin M, Cataland S, Bissell M, Wu HM. A rapid test for the diagnosis of thrombotic thrombocytopenic purpura using surface enhanced laser desorption/ionization time-of-flight (SELDI-TOF)-mass spectrometry. *J Thromb Haemost.* 2006; **4**: 333-338.
- 37) Fujimura Y, Matsumoto M, Yagi H, Yoshioka A, Matsui T, Titani K. Von Willebrand factor-cleaving protease and Upshaw-Schulman syndrome. *Int J Hematol.* 2002; **75**: 25-34.
- 38) 非典型溶血性尿毒症症候群診断基準作成委員会. 非典型溶血性尿毒症症候群 診断基準. *日腎会誌.* 2013; **55**: 91-93.
- 39) 藤村吉博. Upshaw-Schulman 症候群—仮面血小板減少症. *日小児会誌.* 2006; **110**: 1491-1504.
- 40) Schulman I, Pierce M, Likens A, Currimbhoy Z. Studies on thrombopoiesis. I. A factor in normal human plasma required for platelet production; chronic thrombocytopenia due to its deficiency. *Blood.* 1960; **14**: 943-957.
- 41) Upshaw JD Jr. Congenital deficiency of a factor in normal plasma that reverses microangiopathic hemolysis and thrombocytopenia. *N Engl J Med.* 1978; **298**: 1350-1352.
- 42) Kinoshita S, Yoshioka A, Park YD, et al. Upshaw-Schulman syndrome revisited: a concept of congenital thrombotic thrombocytopenic purpura. *Int J Hematol.* 2001; **74**: 101-108.
- 43) Miyata T, Kokame K, Matsumoto M, Fujimura Y. ADAMTS13 activity and genetic mutations in Japan. *Hemostaseologie.* 2013; **33**: 131-137.
- 44) Taguchi F, Yagi H, Matsumoto M, et al. The homozygous p.C1024R-ADAMTS13 gene mutation links to a late-onset phenotype of Upshaw-Schulman syndrome in Japan. *Thromb Haemost.* 2012; **107**: 1003-1005.
- 45) Fujimura Y, Matsumoto M, Isonishi A, et al. Natural history of Upshaw-Schulman syndrome based on ADAMTS13 gene analysis in Japan. *J Thromb Haemost.* 2011; **9 Suppl 1**: 283-301.
- 46) Pos W, Crawley JT, Fijnheer R, Voorberg J, Lane DA, Luken BM. An autoantibody epitope comprising residues R660, Y661, and Y665 in the ADAMTS13 spacer domain identifies a binding site for the A2 domain of VWF. *Blood.* 2010; **115**: 1640-1649.
- 47) Pos W, Sorvillo N, Fijnheer R, et al. Residues Arg568 and Phe592 contribute to an antigenic surface for anti-ADAMTS13 antibodies in the spacer domain. *Haematologica.* 2011; **96**: 1670-1677.
- 48) Matsumoto M, Yagi H, Ishizashi H, Wada H, Fujimura Y. The Japanese experience with thrombotic thrombocytopenic purpura-hemolytic uremic syndrome. *Semin Hematol.* 2004; **41**: 68-74.
- 49) Tun NM, Villani GM. Efficacy of rituximab in acute refractory or chronic relapsing non-familial idiopathic thrombotic thrombocytopenic purpura: a systematic review with pooled data analysis. *J Thromb Thrombolysis.* 2012; **34**: 347-359.
- 50) Froissart A, Buffet M, Veyradier A, et al. French Thrombotic Microangiopathies Reference Center. Efficacy and safety of first-line rituximab in severe, acquired thrombotic thrombocytopenic purpura with a suboptimal response to plasma exchange. Experience of the French Thrombotic Microangiopathies Reference Center. *Crit Care Med.* 2012; **40**: 104-111.

【 Upshaw-Schulman 症候群の ADAMTS13 遺伝子解析 】

ADAMTS13 genetic analysis of Upshaw-Schulman syndrome

小亀 浩市・樋口(江浦) 由佳

Koichi Kokame

Yuka (Eura) Higuchi

Key words

ADAMTS13, 遺伝子解析,
ダイレクト・シーケンシング, 定量 PCR

要約

von Willebrand 因子切断酵素 ADAMTS13 の活性著減は、血栓性血小板減少性紫斑病 (TTP) の発症につながる。常染色体劣性遺伝形式を示す先天性 TTP は Upshaw-Schulman 症候群 (USS) と呼ばれ、ADAMTS13 遺伝子異常が原因となる。我々はこれまで、臨床的に USS が強く疑われた 49 患者に対してダイレクト・シーケンシング法を実施し、46 患者に複合ヘテロあるいはホモ接合性の原因変異を同定した。残り 3 患者のうち 2 患者には 1 アレルのみ変異が検出された。これら 3 患者に対してゲノム定量 PCR 法を行った結果、2 患者に 1,782 bp あるいは 729 bp の欠失を見出した。ダイレクト・シーケンシング法で異常が全く検出されなかった 1 患者では、ゲノム定量 PCR 法でも正常であった。USS の遺伝子解析においてはダイレクト・シーケンシング法が最も効率よく、それで変異が確定しなかった場合、ゲノム定量 PCR 法が有効になると思われる。

1. Upshaw-Schulman 症候群

血栓性血小板減少性紫斑病 (Thrombotic Thrombocytopenic Purpura: TTP) は、血小板減少と溶血性貧血を呈し、時に腎障害や発熱、動揺性精神神経障害を併発する全身性の疾患である。TTP の病態は溶血性尿毒症症候群と類似しており、両者とも血栓性微小血管障害症に属するが、TTP は von Willebrand 因子 (VWF) 切断酵素 ADAMTS13 の活性が著減している点で特徴づけられる。TTP の大半を占める後天性 TTP

の患者血漿には、ADAMTS13 活性を阻害する自己抗体 (インヒビター) が検出される。一方、先天性 TTP では ADAMTS13 遺伝子の異常が原因で ADAMTS13 活性が著減する¹⁾。先天性 TTP は Upshaw-Schulman 症候群 (USS) と呼ばれ、先天性 ADAMTS13 欠損症とほぼ同義である。

ADAMTS13 は VWF マルチマーを切断することで血小板凝集を調節する血漿プロテアーゼであり、その活性が低下すると高分子量 VWF マルチマーの断片化が不十分となる。VWF マルチマーは分子量が大きいほど高い血小板凝集能をもつため、その断片化不全は血小板血栓の形成につながる²⁾。

日本における TTP 診断ガイドラインは未完成であるが、これまでの研究などから、5 徴候 (血小板減少・溶血性貧血・腎障害・発熱・動揺性精神神経障害) が揃っていれば TTP と診断され、5 徴候が揃っていても、血小板減少と溶血性貧血に加え、血漿 ADAMTS13 活性が 5-10% 未満で、インヒビターが陽性であれば後天性 TTP、陰性であれば USS と診断される。USS を確定するには、2 回以上の検査で常に ADAMTS13 活性が低くインヒビターが検出されないことや、家族歴から遺伝性が疑われることなどが重要である。ADAMTS13 遺伝子異常の確認は確定診断の支持に大きく寄与する。

2. ADAMTS13 の構造

ヒトゲノムには ADAMTS (A Disintegrin And Metalloproteinase with Thrombospondin type I motif) ファミリー遺伝子が 19 個存在する。いずれもプロテアー

国立循環器病研究センター 分子病態部

Department of Molecular Pathogenesis, National Cerebral and Cardiovascular Center

〒565-8565 大阪府吹田市藤白台 5-7-1 TEL: 06-6833-5012 (内線 2460)

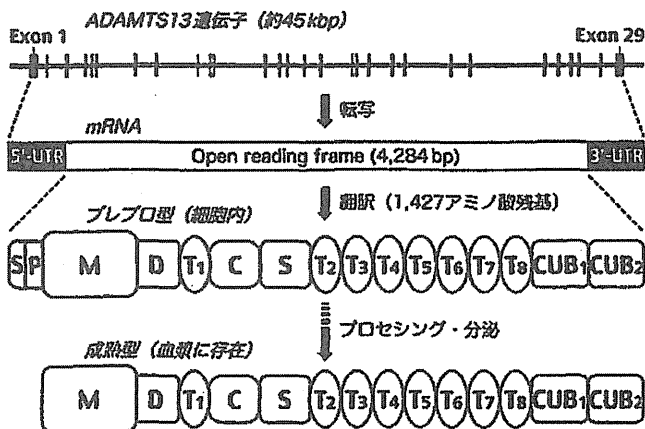


図1 ADAMTS13の遺伝子構造および蛋白質ドメイン構成

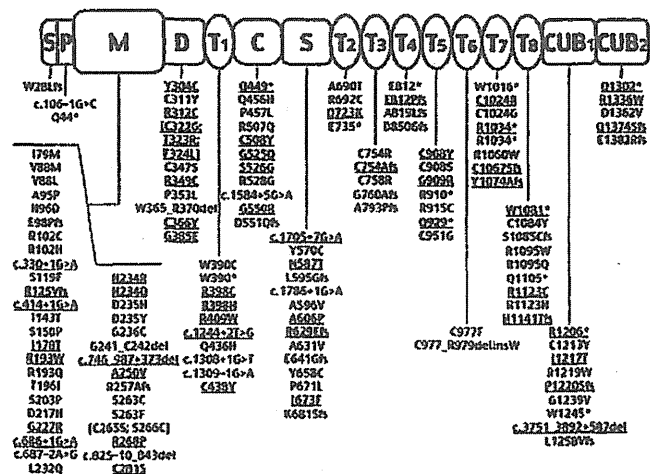


図2 ADAMTS13に同定されたUSF1原因変異。下線は日本人に同定された変異。

でであり、細胞外マトリクスの構築や分解、血管新生、生殖、臓器形成などに関与するが、それぞれの分子機能には不明な点が多い。

ADAMTS13 遺伝子は染色体 9q34 に位置し、約 45 kbp におよぶ 29 個のエクソンからなる (図 1)¹⁾。翻訳領域 ORF (4,284 bp) の開始コドンは exon 1 に、終止コドンは exon 29 にある。

翻訳されたポリペプチド鎖は 1,427 アミノ酸残基からなり、N 末端にシグナル配列とプロペプチドをもつプレプロ型として翻訳される⁴⁾。血液中の成熟型 ADAMTS13 の N 末端はメタロプロテアーゼ (M) ドメインであり、その C 末端側に D ドメイン、T ドメイン、C ドメイン、S ドメインといった ADAMTS に特徴的な構造が続く。ADAMTS の多くはさらに複数の T ドメインをもち、ADAMTS13 では 7 個連続する。その C 末端側に続く 2 個の CUB ドメインは他の ADAMTS がない構造である。

3. ダイレクト・シーケンシング法による変異探索

遺伝子解析を行う場合、まず必要となるのはインフォームド・コンセントの取得や倫理審査委員会での承認などの倫理的手続きである。その後、患者や家族の血液から DNA を抽出し、解析を開始する。USF1 疑い患者の ADAMTS13 遺伝子解析では、すべてのエクソンに対してダイレクト・シーケンシング法による変異探索を行う⁵⁾。ダイレクト・シーケンシング法とは、

検体 DNA を鋳型にして解析対象領域を PCR で増幅し、PCR 産物の塩基配列をサンガー法で直接 (クローニングせずにと意味) 配列決定する方法である。

USF1 は常染色体劣性遺伝形式の疾患であるため、患者は ADAMTS13 遺伝子異常の複合ヘテロ接合体 (各アレルに別の変異) あるいはホモ接合体 (両アレルに同じ変異) である。我々はこれまでに USF1 疑い 49 患者 (43 家系) を解析し、46 患者 (40 家系) に複合ヘテロあるいはホモ接合性の原因変異を同定した。世界的には 140 を超える原因変異が報告されており、我々の報告はその 4 割近くを占める (図 2)。ミスセンス変異が最も多いが、ナンセンス変異やフレームシフト変異、スプライシング異常なども多数報告されている。

我々は患者の遺伝子解析に加え、日本人一般住民の解析も行い、健常者にも見出されるミスセンス多型として、T339R、Q448E、P475S、P618A、S903L、G1181R を同定した⁶⁾。したがって、これらが USF1 患者に見つかっても原因変異とは考えない。ただし、P475S は ADAMTS13 活性を若干低下させる⁷⁾。

4. ゲノム定量 PCR 法による変異探索

USF1 疑い 49 患者のうち 46 患者に複合ヘテロあるいはホモ接合性の原因変異を同定したと述べた。残り 3 患者のうち 2 患者では 1 つの変異しか見つからず、1 患者では全く見つからなかった。そこで、これら 3 患者はダイレクト・シーケンシング法で検出できない変異を

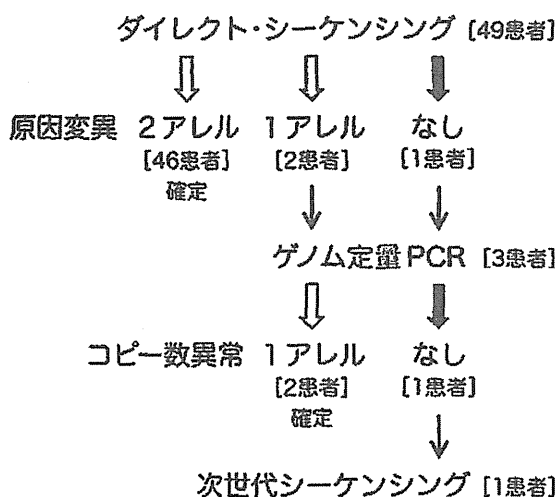


図3 USS患者を対象としたADAMTS13遺伝子解析の流れ

もつと想定した。例えば、あるエクソン領域において一方のアレルは正常で、もう一方のアレルにはPCRプライマーがハイブリダイズできない変異があると、正常アレルのみ増幅される。それをサンガー法で解析すると正常アレルの配列のみが読めるため、両アレルとも正常と誤解される。

そのような弱点を補完するには、ゲノムにおける各エクソンの相対的コピー数を分析することが有効である。その目的でしばしば Multiplex Ligation-dependent Probe Amplification (MLPA) 法やアレイ Comparative Genomic Hybridization (CGH) 法が行われるが、ADAMTS13用の試薬やキットは市販されていない。そこで我々は、エクソン領域ごとに相対的コピー数を分析するゲノム定量PCR法を導入した。さらに、プライマーペアのうち少なくとも一方をダイレクト・シーケンシング法と同じ配列にするという独自の工夫を加えたり。ダイレクト・シーケンシング法と組み合わせれば、エクソン領域の変異を見逃す可能性がなくなり、その点でMLPA法やアレイCGH法にまさる。この解析を行った結果、上述3患者のうち2患者にそれぞれc.746_987+373del (1,782 bp欠失)とc.3751_3892+587del (729 bp欠失)を発見することができた。ADAMTS13遺伝子にこのような長い欠失が見つかったのは初めてである。この2患者にはすでにダイレクト・シーケンシング法でそれぞれp.G550Rとp.C281Sを同定しており、両親の遺伝子解析から、いずれの患者も複合ヘテロ接合体であることが確認された。

おわりに

ダイレクト・シーケンシング法とゲノム定量PCR法を行うことにより、49患者のうち48患者に原因変異を特定することができた(図3)。しかし、残る1患者ではいずれの方法でも異常が見られなかった。現在、次世代シーケンサーを利用して、全イントロンを含むADAMTS13遺伝子全体のシーケンシングを開始したところである。これで新たな変異が見つかるか否か。もし見つからなければ、ADAMTS13遺伝子全体を含む規模の転座や逆位といった異常や、ADAMTS13以外の遺伝子の異常も視野に入れた解析が必要となる。

これまでの経験上、USSのADAMTS13遺伝子解析では、まずダイレクト・シーケンシング法を行うことが効果的であり、9割以上は解決する。原因変異が一つしか見つからない場合、ゲノム定量PCR法で別の変異を発見できる可能性がある。ダイレクト・シーケンシング法で変異が一つも見つからない場合、原因の特定は難渋するかもしれない。

本稿で紹介した成果は、国立循環器病研究センターの宮田敏行部長、奈良県立医科大学の藤村吉博教授、松本雅則准教授ほか、多くの方々との共同研究で得られたものであり、ここに感謝の意を表します。

文献

- 1) Fujimura Y, Matsumoto M, Isonishi A, et al. Natural history of Upshaw-Schulman syndrome based on ADAMTS13 gene analysis in Japan. *J Thromb Haemost* 2011; 9 Suppl 1: 283-301.
- 2) Sadler JE. Von Willebrand factor, ADAMTS13, and thrombotic thrombocytopenic purpura. *Blood* 2008; 112: 11-18.
- 3) Levy GG, Nichols WC, Lian EC, et al. Mutations in a member of the ADAMTS gene family cause thrombotic thrombocytopenic purpura. *Nature* 2001; 413: 488-494.
- 4) Soejima K, Mimura N, Hirashima M, et al. A novel human metalloprotease synthesized in the liver and secreted into the blood: possibly, the von Willebrand factor-cleaving protease? *J Biochem* 2001; 130: 475-480.
- 5) Kokame K, Miyata T. Genetic defects leading to hereditary thrombotic thrombocytopenic purpura. *Seminars in hematology* 2004; 41: 34-40.
- 6) Kokame K, Kokubo Y, Miyata T. Polymorphisms and mutations of ADAMTS13 in the Japanese population and estimation of the number of patients with Upshaw-Schulman syndrome. *J Thromb Haemost* 2011; 9: 1654-1656.
- 7) Akiyama M, Kokame K, Miyata T. ADAMTS13 P475S polymorphism causes a lowered enzymatic activity and urea lability in vitro. *J Thromb Haemost* 2008; 6: 1830-1832.
- 8) Eura Y, Kokame K, Takafuta T, et al. Candidate gene analysis using genomic quantitative PCR: Identification of ADAMTS13 large deletions in two patients with Upshaw-Schulman syndrome. *Mol Genet Genomic Med*; In press.

ORIGINAL ARTICLE *Laboratory science*

Production of functional coagulation factor VIII from iPSCs using a lentiviral vector

Y. KASHIWAKURA,*† T. OHMORI,* J. MIMURO,* S. MADOIWA,* M. INOUE,‡
M. HASEGAWA,‡ K. OZAWA§ and Y. SAKATA*

*Research Division of Cell and Molecular Medicine, Center for Molecular Medicine, Jichi Medical University, Tochigi, Japan;

†Department of Immunology, Dokkyo Medical University School of Medicine, Tochigi, Japan; ‡DNAVEC Corporation, Ibaraki, Japan; and §Division of Genetic Therapeutics, Center for Molecular Medicine, Jichi Medical University, Tochigi, Japan

Summary. The use of induced pluripotent stem cells (iPSCs) as an autologous cell source has shed new light on cell replacement therapy with respect to the treatment of numerous hereditary disorders. We focused on the use of iPSCs for cell-based therapy of haemophilia. We generated iPSCs from mesenchymal stem cells that had been isolated from C57BL/6 mice. The mouse iPSCs were generated through the induction of four transcription factor genes Oct3/4, Klf-4, Sox-2 and c-Myc. The derived iPSCs released functional coagulation factor VIII (FVIII) following transduction with a simian immunodeficiency virus vector. The subcutaneous transplantation of iPSCs expressing FVIII

into nude mice resulted in teratoma formation, and significantly increased plasma levels of FVIII. The plasma concentration of FVIII was at levels appropriate for human therapy at 2–4 weeks post transplantation. Our data suggest that iPSCs could be an attractive and prospective autologous cell source for the production of coagulation factor, and that engineered iPSCs expressing coagulation factor might provide a cell-based therapeutic strategy appropriate for haemophilia.

Keywords: haemophilia, induced pluripotent stem cells, lentiviral vector, cell therapy, gene therapy, blood coagulation

Introduction

Haemophilia is an X-linked inherited bleeding disorder, caused by mutations within the *coagulation factor VIII (F8)* or *coagulation factor IX (F9)* genes. This results in a longer than average time for blood to clot, which can lead to significant bleeding. Haemophilia is considered suitable for gene therapy, as it is caused by a single gene abnormality, and therapeutic coagulation factor levels can vary across a broad range [1]. Recently, therapeutic levels of coagulation factor have been achieved in haemophilia B patients through the direct administration of adeno-associated virus vectors in clinical trials [2]. Another gene therapy strategy for haemophilia is the application of cells transduced *ex vivo*, as a delivery vehicle for coagulation factor [3].

Cell-based therapy reduces the risk of unwanted virus dissemination, and ensures the selection of highly expressing clones prior to commencement of the procedure. However, cell-based therapies for haemophilia have been hampered in animals and during human clinical trials, because of the short life span of transplanted cells, difficulties in obtaining therapeutic plasma levels, and elimination of the transduced cells by immune reactions [4].

Induced pluripotent stem cells (iPSCs) are artificially generated stem cells, made by reprogramming somatic cells through the expression of defined transcription factors [5,6]. These iPSCs are pluripotent, with the ability to differentiate into cells of the three germ lineages *in vitro*. Mouse-derived iPSCs can be passaged through the germ line, as is the case with embryonic stem cells (ESCs). Using iPSCs has a distinct advantage over ESCs, as cells differentiated from iPSCs exhibit limited immunogenicity, and are therefore more easily tolerated by a recipient following transplantation. Accordingly, iPSC technology offers the possibility of patient-specific cell therapy for haemophilia, in which the use of genetically identical cells would prevent immune rejection. In this study, we examined whether iPSCs could release

Correspondence: Tsukasa Ohmori, MD, PhD, Research Division of Cell and Molecular Medicine, Center for Molecular Medicine, Jichi Medical University, 3111-1 Yakushiji, Shimotsuke, Tochigi 329-0498, Japan.

Tel: +81-285-58-7397; fax: +81-285-44-7817;
e-mail: tohmori@jichi.ac.jp

Accepted after revision 7 October 2013

functional coagulation factor using lentiviral transduction. We then focused on the possible clinical application of the engineered iPSCs to cell-based gene therapy for haemophilia.

Materials and methods

Mice

C57BL/6J mice were purchased from Japan SLC (Shizuoka, Japan). BALB/cAJcl-*nu/nu* mice (nude mice) were obtained from CLEA Japan, Inc. (Shizuoka, Japan). All animal procedures were approved by the Institutional Animal Care and Concern Committee at Jichi Medical University, and animal care was in accordance with the committee's guidelines.

Generation of iPSCs and cell culture

Murine mesenchymal stem cells (MSCs) were isolated and maintained as described previously [7]. We selected MSCs for the establishment of iPSCs because MSCs have a higher reprogramming efficiency compared with fibroblasts [8,9]. Two plasmid vectors to generate iPSCs (pCX-OKS-2A and pCX-cMyc) were obtained from Addgene (Cambridge, MA). MSCs were transduced with the plasmid vectors by nucleofection as described previously [10]. Colonies that were ES-like were cloned at 30 days post transduction, and MSC-derived iPSCs were maintained on mouse embryonic fibroblasts with knockout Dulbecco's modified Eagle's medium (DMEM; Invitrogen, Carlsbad, CA) supplemented with 15% foetal bovine serum, 2 mM L-glutamine, 1 mM sodium pyruvate, 0.1 mM non-essential amino acids, 0.5 mM monothio-glycerol (Wako Pure Chemical Industries, Ltd., Osaka, Japan) and 1000 U mL⁻¹ ESGRO (Merck Millipore, Billerica, MA).

Reverse transcription polymerase chain reaction (RT-PCR)

Total RNA was prepared using an RNeasy Mini Kit (QIAGEN, Montgomery, MD). The RT-PCR assays were conducted using a SuperScript One-Step RT-PCR System (Invitrogen). Primer pairs for the RT-PCR assays used in this study have been previously reported [5].

Lentiviral vector construct and production

The cDNA for human B-domain-deleted FVIII (hBDD-FVIII) was generated as previously described [11]. The *hBDD-FVIII* gene, under the control of a chicken β -actin promoter coupled with cytomegalovirus promoter early enhancer element (CAGp), was

cloned into a self-inactivating simian immunodeficiency virus (SIV) lentiviral vector [12]. The SIV lentiviral vectors were generated as previously described [13].

Measurement of FVIII activity and antigen

The hFVIII antigens (FVIII:Ag) were measured using an anti-hFVIII-specific enzyme-linked immunosorbent assay (ELISA) kit (ASSERACHROM VIII:Ag; Diagnostica Stago, Seine, France). The functional activity of FVIII (FVIII:C) was measured using a one-stage clotting time assay on an automated coagulation analyser (Sysmex CA-500 analyser; Sysmex Corp., Kobe, Japan). We used pooled normal human plasma as a reference to measure both FVIII:C and FVIII:Ag.

Results and discussion

We first attempted to establish iPSCs from C57BL/6 mice. Bone marrow-derived MSCs were transduced with plasmid vector expressing the defined transcription factors. We cloned ESC-like cell colonies after transduction, and SSEA-1 positive cells were sorted by flow cytometry (Fig. 1a). The sorted cell colonies exhibited typical ESC morphology and alkaline phosphatase activity (Fig. 1b). The mRNA expression patterns of endogenous pluripotent-specific genes (*Sox2*, *Oct3/4*, *Nanog* and *c-Myc*) in the cells were similar to those in E14tg2a mouse ESCs (Fig. 1c). Furthermore, subcutaneous transplantation of these cells (1×10^6 cells) into nude mice resulted in the formation of teratomas containing tissues derived from the ectoderm, mesoderm, and endoderm (Fig. 1d and e). This would suggest that the cells possess the potential to differentiate into cells and tissues of the three germ layers. Therefore, we used these iPSCs for further experiments in this study.

We next examined whether iPSCs could produce functional coagulation factor after transduction by a lentiviral vector. The iPSCs were transduced with the SIV vector expressing hBDD-FVIII under the control of CAGp (SIV-CAG-hFVIII) (Fig. 2a). We cloned iPSC colonies from the cells transduced with SIV-CAG-hFVIII at a multiplicity of infection (MOI) of 30, and selected three iPSC clones that stably produced hFVIII in the supernatant (Fig. 2b). The iPSC clones expressing hFVIII were subcutaneously transplanted into nude mice. Following transplantation, plasma levels of hFVIII:Ag in nude mice gradually increased according to teratoma formation derived from the transplanted iPSCs (Fig. 2c and d). Although the plasma level of hFVIII:Ag in the nude mice was at 20%, we could not measure hFVIII:C in nude mice because of the existence of mouse FVIII. We simultaneously measured hFVIII:C and hFVIII:Ag produced from transduced

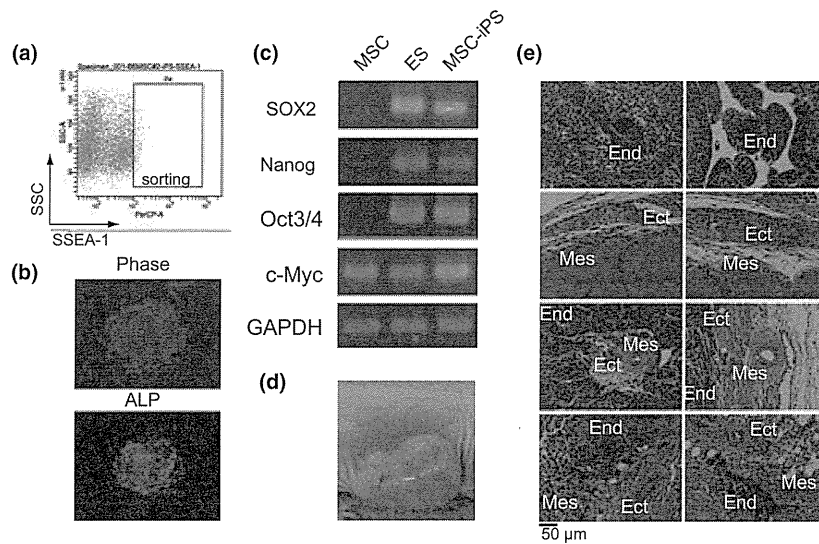


Fig. 1. Characterization of induced pluripotent stem cells (iPSCs) derived from mesenchymal stem cells (MSCs). MSCs isolated from C57BL/6 mice were transduced with plasmid vectors expressing Oct3/4, Klf4, Sox2 and c-Myc. (a) Stage-specific embryonic antigen 1 (SSEA-1) expression was examined by flow cytometry following transduction. SSEA-1-positive cells (shown in the square) were sorted as MSC-derived iPSCs. (b) Morphology of iPSC colonies derived from SSEA-1-positive cells. Alkaline phosphatase activity in iPSC colonies was detected using HNP/Fast Red TR. (c) The mRNA expression levels of the pluripotency markers SOX2, Nanog, Oct3/4 and c-Myc were determined by reverse transcription polymerase chain reaction. (d) Teratoma formation in nude mice after subcutaneous transplantation of iPSCs. (e) Differentiation into cells and tissues of the three germ lineages were confirmed by histological analysis. End, endoderm; Ect, ectoderm; Mes, mesoderm.

iPSCs, and calculated the ratio of hFVIII:C to hFVIII:Ag (0.30 ± 0.041). Accordingly, hFVIII:C levels seemed to reach the therapeutic level of FVIII required for haemophilia A (6%) in transplanted mice.

Recent studies have reported the potential of iPSCs for the treatment of many human diseases; iPSCs possess the ability to differentiate into cardiovascular [14–16], haematopoietic [16,17], neural [18], and hepatic [19,20] progenitor cells. Treatment of inherited disorders using iPSCs has been proposed for animal models of sickle cell anaemia [17]. The haemophilic mouse model could also be used to examine the potential of iPSC therapy. Xu *et al.* reported that transplantation of endothelial progenitor cells derived from iPSCs into the liver increased FVIII levels, resulting in a corrected bleeding phenotype for haemophilia A mice [21,22]. The results reported by Xu *et al.* were surprising because the differentiated endothelial progenitor cells that were transplanted only contained one copy of *F8*, yet they were able to increase plasma levels of FVIII. In contrast, lentiviral transduction using our procedure resulted in 5–10 proviral integration sites in the diploid genome at an MOI of 30, suggesting that the same procedure using engineered iPSCs expressing coagulation factor would result in a more potent therapeutic effect.

In our preliminary experiments, we used nude mice to verify the following: the net production of FVIII from iPSCs by excluding the role of the immune system; and pluripotency of iPSCs by teratoma formation. However, tumourigenesis by iPSCs, should be

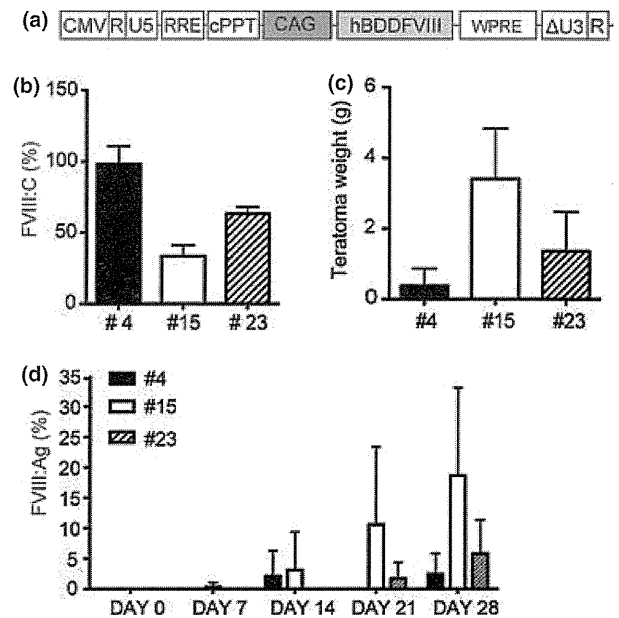


Fig. 2. Increase in FVIII levels after transduction with the simian immunodeficiency virus (SIV) lentiviral vector. The induced pluripotent stem cells (iPSCs) were transduced with SIV vector expressing human B-domain deleted coagulation factor VIII (hBDD-FVIII) under the control of a CAG promoter (SIV-CAG-hFVIII) at an MOI of 30. (a) Schematic of the SIV vectors used in our experiments. (b) FVIII activities in the supernatants derived from cloned iPSCs (#4, #15, and #23) transduced with SIV-CAG-hFVIII were measured using a one-stage clotting time assay. Values are presented as means \pm SD ($n = 4$ for each experiment). (c, d) iPSC clones expressing hFVIII were subcutaneously transplanted into nude mice. (c) Teratoma weight at 4 weeks after subcutaneous transplantation of cloned MSC-iPSCs transduced with SIV-CAG-hFVIII. Values are presented as means \pm SD ($n = 3-5$). (d) Plasma FVIII antigen levels in nude mice at the indicated times after subcutaneous transplantation of the iPSC clones. Values are means \pm SD ($n = 3-5$).

completely avoided in their application. To reduce tumourigenicity and to improve the safety of iPSCs, the use of non-integrative vectors and changes of defined factors has been widely examined [6,23–25]. We also should differentiate iPSCs into the appropriate cells before transplantation, and plan to establish a more realistic cell therapy approach using immunocompetent FVIII-deficient mice.

One strategy to increase the safety of iPSCs for cell therapy would be to administer anucleated cells, such as red blood cells and platelets, differentiated from iPSCs. Integration of transgenes into genomic DNA during iPSC induction and lentiviral transduction might be negligible in the transplantation of anucleate cells. We have previously reported, along with other researchers, that expression of coagulation factor in red blood cells [26] and platelets [13,27] using lentiviral vectors has corrected the phenotype of mouse models of haemophilia. The use of blood cells to deliver coagulation factor is attractive as it avoids interference from circulating inhibitors. Recent reports have suggested the production of functional platelets from human iPSCs [28]; the transfusion of these blood cells expressing coagulation factor produced from iPSCs *in vitro* is possibly the most efficient and effective method for treating haemophiliacs.

In conclusion, we have proposed a new cell-based treatment for haemophilia involving iPSCs. Our proposed approach appears to be feasible, as transplantation of iPSCs resulted in increased and therapeutically appropriate FVIII plasma levels. Further investigations are needed to explore the risks of tumourigenicity from iPSC-derived cells, and to efficiently increase plasma levels of coagulation factor following cell therapy.

Acknowledgements

Y. Kashiwakura and T. Ohmori designed and performed the experiments, analysed the data and wrote the manuscript; M. Inoue and M. Hasegawa provided vital reagents and critically reviewed the manuscript; and J. Mimuro, S. Madoiwa, K. Ozawa and Y. Sakata analysed the data and revised the manuscript. We thank Naoko Ito and Masanori Ito (Jichi Medical University) for their technical assistance. This study was supported by a Grant from the Japan Baxter Hemophilia Scientific Research & Education Fund; Grants-in-Aid for Scientific Research (23591427, 21591249 and 23591426); Special Project Award from Bayer Hemophilia Award Program 2011; the Support Program for Strategic Research Infrastructure from the Japanese Ministry of Education and Science, and Health, Labour and Science Research Grants for Research on HIV/AIDS and Research on Intractable Diseases from the Japanese Ministry of Health, Labour and Welfare.

Disclosures

The authors stated that they had no interests that might be perceived as posing a conflict or bias.

References

- Mannucci PM, Tuddenham EG. The hemophilias—from royal genes to gene therapy. *N Engl J Med* 2001; **344**: 1773–9.
- Nathwani AC, Tuddenham EG, Rangarajan S *et al*. Adenovirus-associated virus vector-mediated gene transfer in hemophilia B. *N Engl J Med* 2011; **365**: 2357–65.
- Lillicrap D, VandenDriessche T, High K. Cellular and genetic therapies for haemophilia. *Haemophilia* 2006; **12**(Suppl 3): 36–41.
- Roth DA, Tawa NE Jr., O'Brien JM, Treco DA, Selden RF. Nonviral transfer of the gene encoding coagulation factor VIII in patients with severe hemophilia A. *N Engl J Med* 2001; **344**: 1735–42.
- Takahashi K, Yamanaka S. Induction of pluripotent stem cells from mouse embryonic and adult fibroblast cultures by defined factors. *Cell* 2006; **126**: 663–76.
- Okita K, Ichisaka T, Yamanaka S. Generation of germline-competent induced pluripotent stem cells. *Nature* 2007; **448**: 313–7.
- Kashiwakura Y, Ohmori T, Mimuro J *et al*. Intra-articular injection of mesenchymal stem cells expressing coagulation factor ameliorates hemophilic arthropathy in factor VIII-deficient mice. *J Thromb Haemost* 2012; **10**: 1802–13.
- Niibe K, Kawamura Y, Araki D *et al*. Purified mesenchymal stem cells are an efficient source for iPS cell induction. *PLoS ONE* 2011; **6**: e17610.
- Oda Y, Yoshimura Y, Ohnishi H *et al*. Induction of pluripotent stem cells from human third molar mesenchymal stromal cells. *J Biol Chem* 2010; **285**: 29270–8.
- Gonzalez F, Barragan Monasterio M, Tiscornia G *et al*. Generation of mouse-induced pluripotent stem cells by transient expression of a single nonviral polycistronic vector. *Proc Natl Acad Sci USA* 2009; **106**: 8918–22.
- Ogata K, Mimuro J, Kikuchi J *et al*. Expression of human coagulation factor VIII in adipocytes transduced with the simian immunodeficiency virus agmTYO1-based vector for hemophilia A gene therapy. *Gene Ther* 2004; **11**: 253–9.
- Nakajima T, Nakamaru K, Ido E, Terao K, Hayami M, Hasegawa M. Development of novel simian immunodeficiency virus vectors carrying a dual gene expression system. *Hum Gene Ther* 2000; **11**: 1863–74.
- Ohmori T, Mimuro J, Takano K *et al*. Efficient expression of a transgene in platelets using simian immunodeficiency virus-based vector harboring glycoprotein Ibalph promoter: in vivo model for platelet-targeting gene therapy. *FASEB J* 2006; **20**: 1522–4.
- Kuzmenkin A, Liang H, Xu G *et al*. Functional characterization of cardiomyocytes derived from murine induced pluripotent stem cells in vitro. *FASEB J* 2009; **23**: 4168–80.
- Narazaki G, Uosaki H, Teranishi M *et al*. Directed and systematic differentiation of cardiovascular cells from mouse induced pluripotent stem cells. *Circulation* 2008; **118**: 498–506.
- Schenke-Layland K, Rhodes KE, Angelis E *et al*. Reprogrammed mouse fibroblasts differentiate into cells of the cardiovascular and hematopoietic lineages. *Stem Cells* 2008; **26**: 1537–46.
- Hanna J, Wernig M, Markoulaki S *et al*. Treatment of sickle cell anemia mouse model with iPS cells generated from autologous skin. *Science* 2007; **318**: 1920–3.
- Wernig M, Zhao JP, Pruszak J *et al*. Neurons derived from reprogrammed fibroblasts functionally integrate into the fetal brain and improve symptoms of rats with Parkinson's disease. *Proc Natl Acad Sci USA* 2008; **105**: 5856–61.
- Cantz T, Bleidissel M, Stehling M, Scholer HR. In vitro differentiation of reprogrammed murine somatic cells into hepatic precursor cells. *Biol Chem* 2008; **389**: 889–96.
- Kasuda S, Tatsumi K, Sakurai Y *et al*. Expression of coagulation factors from murine induced pluripotent stem cell-derived liver cells. *Blood Coagul Fibrinolysis* 2011; **22**: 271–9.
- Xu D, Alipio Z, Fink LM *et al*. Phenotypic correction of murine hemophilia A using an iPS cell-based therapy. *Proc Natl Acad Sci USA* 2009; **106**: 808–13.
- Alipio Z, Adcock DM, Waner M *et al*. Sustained factor VIII production in hemophilic mice 1 year after engraftment with induced pluripotent stem cell-derived factor VIII producing endothelial cells. *Blood Coagul Fibrinol* 2010; **21**: 502–4.
- Kaji K, Norrby K, Paca A, Mileikovsky M, Mohseni P, Woltjen K. Virus-free induction of pluripotency and subsequent excision of reprogramming factors. *Nature* 2009; **458**: 771–5.

- 24 Zhou H, Wu S, Joo JY *et al.* Generation of induced pluripotent stem cells using recombinant proteins. *Cell Stem Cell* 2009; 4: 381–4.
- 25 Fusaki N, Ban H, Nishiyama A, Saeki K, Hasegawa M. Efficient induction of transgene-free human pluripotent stem cells using a vector based on Sendai virus, an RNA virus that does not integrate into the host genome. *Proc Jpn Acad Ser B Phys Biol Sci* 2009; 85: 348–62.
- 26 Chang AH, Stephan MT, Sadelain M. Stem cell-derived erythroid cells mediate long-term systemic protein delivery. *Nat Biotechnol* 2006; 24: 1017–21.
- 27 Shi Q, Wilcox DA, Fahs SA *et al.* Lentivirus-mediated platelet-derived factor VIII gene therapy in murine haemophilia A. *J Thromb Haemost* 2007; 5: 352–61.
- 28 Takayama N, Nishimura S, Nakamura S *et al.* Transient activation of c-MYC expression is critical for efficient platelet generation from human induced pluripotent stem cells. *J Exp Med* 2010; 207: 2817–30.

OP9 Bone Marrow Stroma Cells Differentiate into Megakaryocytes and Platelets

Yumiko Matsubara^{1*}, Yukako Ono², Hidenori Suzuki³, Fumio Arai⁴, Toshio Suda⁴, Mitsuru Murata¹, Yasuo Ikeda⁵

1 Department of Laboratory Medicine, Keio University School of Medicine, Tokyo, Japan, **2** Division of Hematology, Department of Medicine, Keio University School of Medicine, Tokyo, Japan, **3** Department of Morphological and Biomolecular Research, Nippon Medical School, Tokyo, Japan, **4** Department of Cell Differentiation, Keio University School of Medicine, Tokyo, Japan, **5** Faculty of Science and Engineering, Life Science and Medical Bioscience, Waseda University, Tokyo, Japan

Abstract

Platelets are essential for hemostatic plug formation and thrombosis. The mechanisms of megakaryocyte (MK) differentiation and subsequent platelet production from stem cells remain only partially understood. The manufacture of megakaryocytes (MKs) and platelets from cell sources including hematopoietic stem cells and pluripotent stem cells have been highlighted for studying the platelet production mechanisms as well as for the development of new strategies for platelet transfusion. The mouse bone marrow stroma cell line OP9 has been widely used as feeder cells for the differentiation of stem cells into MK lineages. OP9 cells are reported to be pre-adipocytes. We previously reported that 3T3-L1 pre-adipocytes differentiated into MKs and platelets. In the present study, we examined whether OP9 cells differentiate into MKs and platelets using MK lineage induction (MKLI) medium previously established to generate MKs and platelets from hematopoietic stem cells, embryonic stem cells, and pre-adipocytes. OP9 cells cultured in MKLI medium had megakaryocytic features, i.e., positivity for surface markers CD41 and CD42b, polyploidy, and distinct morphology. The OP9-derived platelets had functional characteristics, providing the first evidence for the differentiation of OP9 cells into MKs and platelets. We then analyzed gene expressions of critical factors that regulate megakaryopoiesis and thrombopoiesis. The gene expressions of p45NF-E2, FOG, Fli1, GATA2, RUNX1, thrombopoietin, and c-mpl were observed during the MK differentiation. Among the observed transcription factors of MK lineages, p45NF-E2 expression was increased during differentiation. We further studied MK and platelet generation using p45NF-E2-overexpressing OP9 cells. OP9 cells transfected with p45NF-E2 had enhanced production of MKs and platelets. Our findings revealed that OP9 cells differentiated into MKs and platelets *in vitro*. OP9 cells have critical factors for megakaryopoiesis and thrombopoiesis, which might be involved in a mechanism of this differentiation. p45NF-E2 might also play important roles in the differentiation of OP9 cells into MK lineage cells.

Citation: Matsubara Y, Ono Y, Suzuki H, Arai F, Suda T, et al. (2013) OP9 Bone Marrow Stroma Cells Differentiate into Megakaryocytes and Platelets. PLoS ONE 8(3): e58123. doi:10.1371/journal.pone.0058123

Editor: Linzhao Cheng, Johns Hopkins Univ. School of Medicine, United States of America

Received: September 18, 2012; **Accepted:** January 31, 2013; **Published:** March 1, 2013

Copyright: © 2013 Matsubara et al. This is an open-access article distributed under the terms of the Creative Commons Attribution License, which permits unrestricted use, distribution, and reproduction in any medium, provided the original author and source are credited.

Funding: This work was supported by the Grants-in-Aid from the Ministry of Education, Culture, Sports, Science, and Technology of Japan (<http://www.mext.go.jp/>) (#21591250 to Y. Matsubara and #22659183 to Y. Ikeda and Y. Matsubara) and from the Japanese Ministry of Health Labor and Welfare (<http://www.mhlw.go.jp/>) for blood coagulation abnormalities (to M. Murata). The funders had no role in study design, data collection and analysis, decision to publish, or preparation of the manuscript.

Competing Interests: The authors have declared that no competing interests exist.

* E-mail: yumikoma@a7.keio.jp

Introduction

Platelets play critical roles in hemostatic plug formation and thrombosis [1–3]. Platelets are released from terminally differentiated megakaryocytes (MKs). The underlying molecular mechanisms of megakaryopoiesis and subsequent thrombopoiesis are only partially understood [4–10]. Current advances in a culture system to generate MKs and platelets *in vitro* help us to clarify the mechanism underlying MK differentiation and platelet production [11]. Also, studies on new strategies to manufacture MKs and platelets pursue to develop a donor-independent source for platelet transfusion [11].

MKs and platelets have been differentiated from hematopoietic stem cells (HSCs), embryonic stem (ES) cells, fetal liver cells, induced pluripotent stem (iPS) cells, and fibroblasts transfected with a combination of p45NF-E2, Maf G, and Maf K, *in vitro* [12–19]. Moreover, we reported the generation of MKs and functional

platelets from both normal human subcutaneous adipose tissues and mouse pre-adipocyte cell line 3T3-L1 [20–22]. Differentiation of pre-adipocytes into MKs and platelets has been observed when the culture medium is switched from maintenance medium to MK lineage induction (MKLI) medium previously established to generate platelets from HSCs and ES cells [21–24].

The mouse bone marrow stroma cell line OP9 was established from macrophage colony stimulating factor deficient osteopetrotic mice [25]. OP9 cells have been widely used as feeder cells for the differentiation of ES cells and iPS cells into hematopoietic cells as well as for the differentiation of these stem cells into MKs and platelets [12–15, 25–27]. Also, OP9 cells were reported to be pre-adipocytes [28, 29]. In the present study, we examined whether OP9 cells differentiate MKs and platelets, based on our previous observations that pre-adipocytes differentiated into MKs and platelets [20–22], and then investigated the involved mechanisms of MK differentiation and platelet production from OP9 cells.

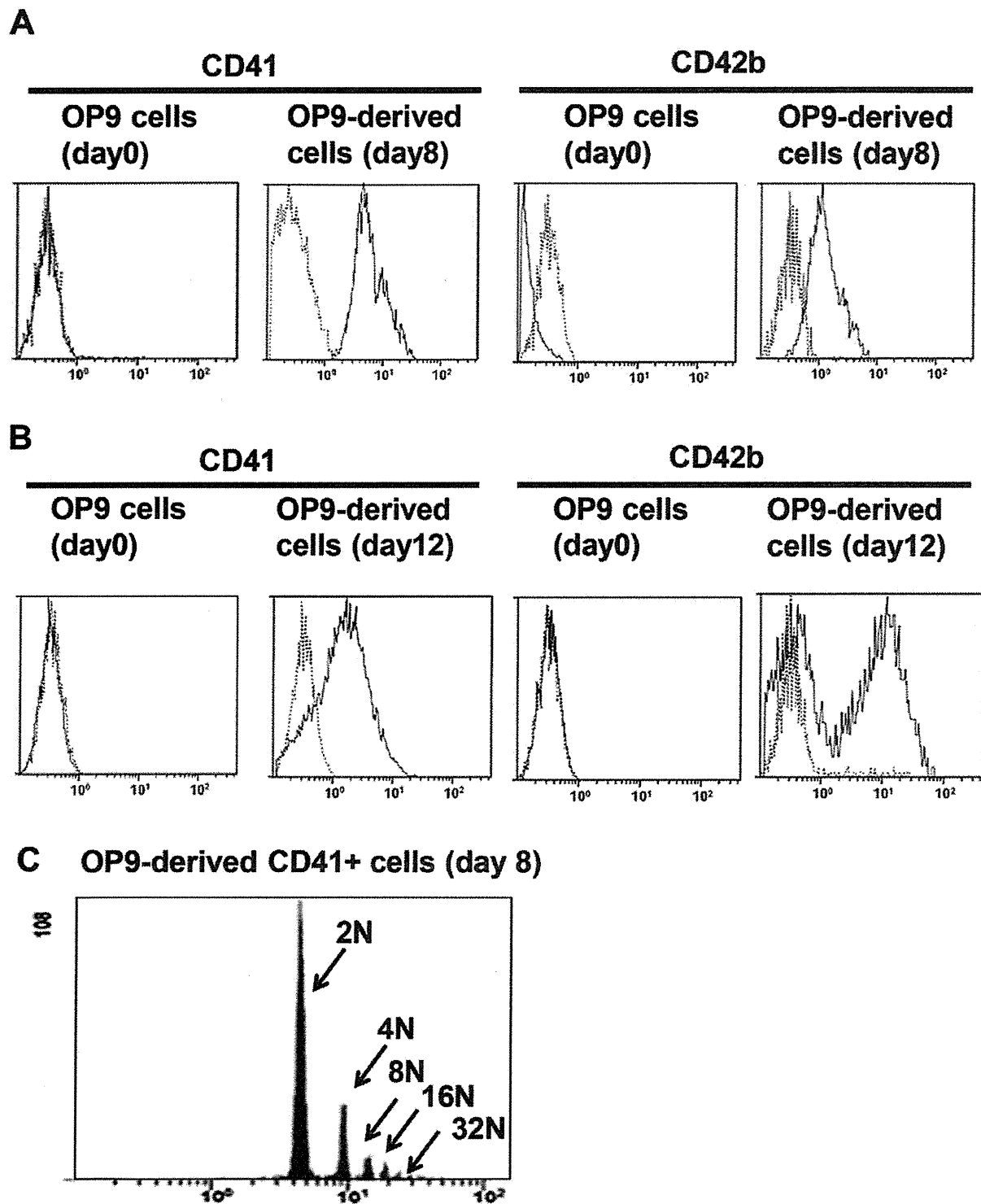


Figure 1. Flow cytometric analyses for megakaryocytes and platelets differentiated from OP9 cells. **A**, Representative flowcytometry histogram of CD41 and CD42b expression on megakaryocyte-sized cells. Dot-line shows data using isotype control. **B**, Representative flowcytometry histogram of CD41 and CD42b expression on platelet-sized cells. Dot-line shows data using isotype control. **C**, DNA ploidy analysis in OP9-derived CD41+ cells on day 8.
doi:10.1371/journal.pone.0058123.g001

Methods

Cell Culture for Differentiation into MKs and Platelets

OP9 cells were maintained as described previously [12]. To induce the differentiation of OP9 cells into MK lineages, OP9 cells were cultured for 12 to 14 days using MKLI medium comprised of Iscove's Modified Dulbecco's Medium supplemented with 2 mM L-glutamine, 100 U/ml penicillin G sodium, 0.1 mg/ml streptomycin sulfate, 0.5% bovine serum albumin, 4 µg/ml LDL cholesterol, 200 µg/ml iron-saturated transferrin, 10 µg/ml insulin, 50 µM 2-β-mercaptoethanol, 20 µM each nucleotide (ATP, UTP, GTP, and CTP), and 50 ng/ml thrombopoietin (TPO; a gift from Kyowa Hakko Kirin CO., Ltd.) [19–24]. Mouse ES cells (gifted by Dr. Niwa H, RIKEN Center, Kobe, Japan) were established as described previously [30]. We maintained the ES cells as described previously [21,31]. Primary mouse low-density bone marrow mononuclear cells (mBMMNCs) were obtained as described previously [23] and were then cultured in MKLI medium.

Flow Cytometric Analyses

Surface marker analyses were performed on OP9 cells before the MK induction (day 0) and OP9 cells cultured in MKLI medium (OP9-derived cells). We used the directly labeled

fluorescein isothiocyanate (FITC)-conjugated antibodies for CD41 (also known as platelet glycoprotein IIb) (BD bioscience), and CD42b (also known as platelet glycoprotein Ib alpha) (EMFRET Analytics GmbH and Co.). The positive values (%) were calculated using cell number of binding to isotype control and cell number of binding to anti-CD41-antibody or anti-CD42b-antibody. Fluorescence-activated cell sorting was used to obtain CD41+ population from OP9-derived cells. OP9-derived MKs and platelets were counted as large-sized CD41+ cells and small-sized CD41+ cells, respectively [23]. The “platelet-sized” particles were defined using mouse platelets, and the plot is shown in Figure S1. DNA ploidy was assessed by interaction with propidium iodide (Sigma) as described previously [22].

Morphologic Analyses

The ultrastructure for OP9-derived CD41+ cells on day 8 and mouse bone marrow cells was analyzed. These studies were done by transmission electron microscopy as described previously [32]. To examine proplatelet formation in OP9-derived cells, the OP9-derived CD41+ cells were plated on the fibrinogen-coated glass (100 µg/ml) were incubated for 6 hours at 37 degree C. These cells were observed using scanning electron microscopy as described previously [33]. Also, the cells were fixed with 4% paraformaldehyde in Ca⁺⁺- and Mg⁺⁺-free Phosphate Buffered

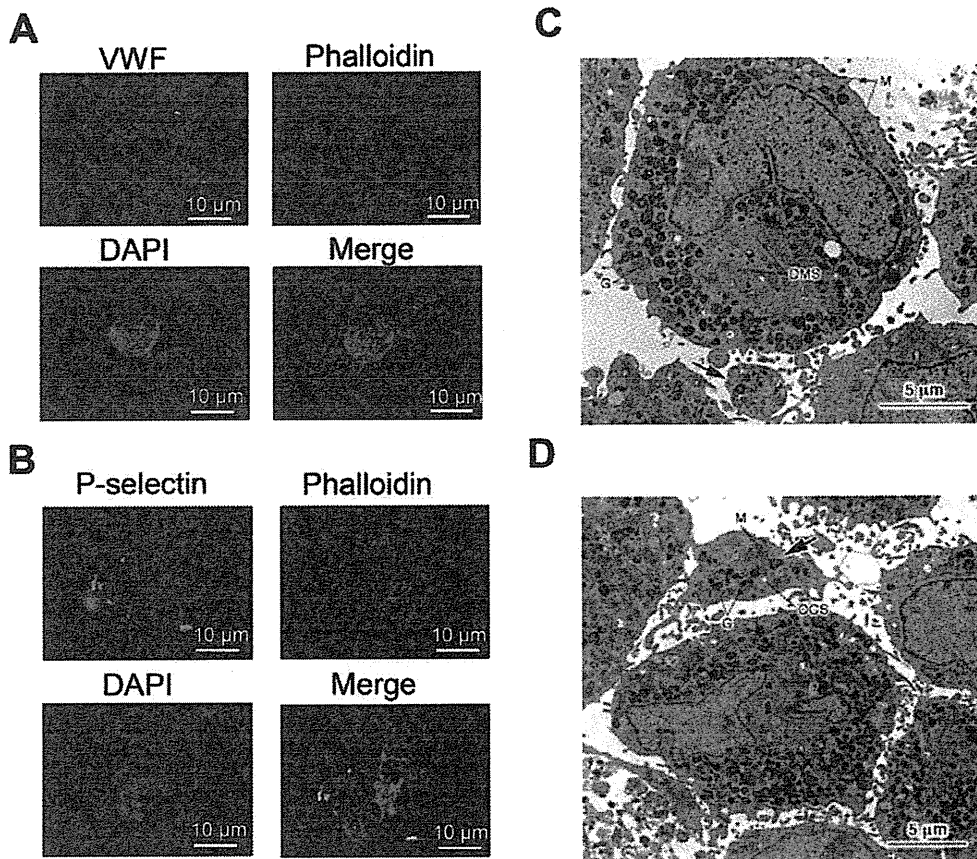


Figure 2. Cell staining and morphologic analyses. **A**, Cells stained with antibody for von Willebrand factor (green), Phalloidin (red) and DAPI (blue). **B**, Cells stained with antibody for P-selectin (green), Phalloidin (red) and DAPI (blue). **C, D**, Transmission electron micrograph of OP9-derived CD41+ cells. Megakaryocyte and platelet (arrow indicated in black): G, granule, DMS, demarcation membrane system, M, mitochondria, and OCS, open canalicular system.

doi:10.1371/journal.pone.0058123.g002

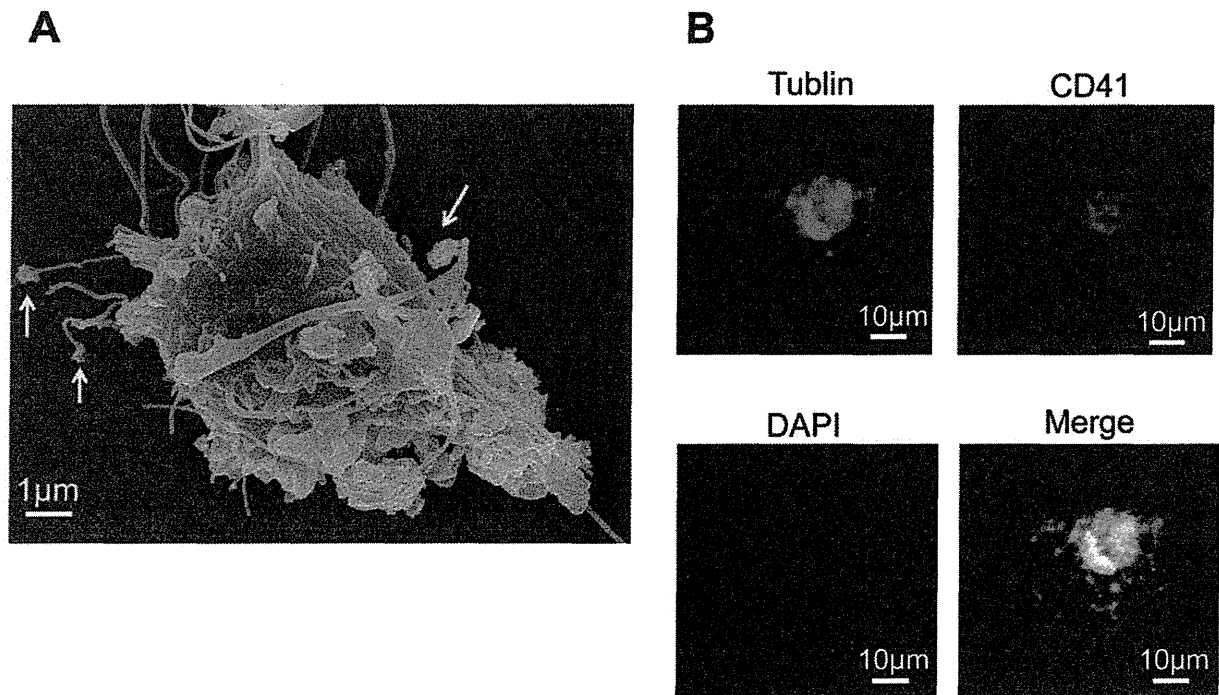


Figure 3. Proplatelet formation in OP9-derived megakaryocyte. **A.** Scanning electron micrograph of proplatelets (arrow indicated in yellow) forming OP9-derived CD41+ cells. **B.** Proplatelet-forming megakaryocyte was stained with antibody for CD41 (red) and alpha-tubulin (green), and DAPI (blue).

doi:10.1371/journal.pone.0058123.g003

Saline (PBS) for 15 minutes at room temperature and then permeabilized by 0.2% Triton X 100 in PBS for 5 minutes at room temperature. The samples for proplatelet formation were stained with phycoerythrin-conjugated antibody for CD41 (BD bioscience), unlabeled anti-alpha-tubulin antibody (Lab Vision Co.) and FITC-conjugated anti-rabbit antibody, and DAPI blue.

Immunohistochemical Studies

To analyze the expression of von Willebrand factor (VWF) and P-selectin in OP9-derived CD41+ cells on day 8, the cells stimulated with 10 μM ADP and 10 μM epinephrine were plated on the fibrinogen-coated glass (100 μg/ml, coating concentration). The cells were fixed with 4% paraformaldehyde in Ca⁺⁺- and Mg⁺⁺-free PBS for 10 minutes at room temperature and then permeabilized by 0.2% Triton X 100 in PBS for 5 minutes at room temperature. The samples from OP9-derived CD41+ cells were stained with FITC-conjugated anti-VWF antibody (EMFRET Analytics GmbH and Co.) and FITC-conjugated anti-P-selectin antibody (EMFRET Analytics GmbH and Co.) for 60 min at room temperature. Cells were also stained DAPI blue and Texas Red Phalloidin (Invitrogen).

Functional Analyses for OP9-derived Platelets

Function for OP9-derived platelets was examined. The analyses of fibrinogen binding and P-selectin surface exposure after stimulation were performed on OP9-derived cells on day 12, as described previously [22]. FITC-conjugated anti-P-selectin antibody (EMFRET Analytics GmbH and Co.) was used for the analysis of P-selectin surface exposure in the presence or absence of stimulation.

Gene Expression Analyses

To carry out gene expression analyses by reverse transcription-polymerase chain reaction (RT-PCR), total RNA samples were prepared from OP9-derived cells on days 0, 4, and 8, mES cells, and mBMMNC-derived cells on days 0 and 4 after treatment with Trizol reagent (Invitrogen). cDNA samples with genomic DNA removal were obtained by QuaniTect Reverse Transcription (QIAGEN) or by QuaniTect Whole Transcriptome (QIAGEN) with DNase (Promega), according to manufacturer's protocols. Primers of RT-PCR for GATA1, GATA2, Fli1, FOG, p45NF-E2, and GAPDH were used as described previously [16]. The pre-made primers (Applied Biosystems) were used for RT-PCR for OCT3/4, SOX2, RUNX1, TPO, c-mpl, KLF1, and PU1. Quantitative real time-PCR was also performed on samples from OP9 cells and OP9-derived cells using pre-made primers (Applied Biosystems). The amount of target normalized to GAPDH was determined by evaluating expression: $2^{-\Delta\Delta Ct}$, where $\Delta\Delta Ct = \Delta Ct_s - \Delta Ct_{cb}$, ΔCt_s was threshold cycle, ΔCt_s was the ΔCt value of a sample, ΔCt_{cb} was that of the calibrator and meant the difference in threshold cycles between the target and reference.

Retroviral Vectors and Cell Culture

Retroviral vector for overexpression of p45NF-E2 in OP9 cells was used as described previously [19]. A CalPhos Mammalian Transfection Kit (Clontech) and AmphiPack-293 cells (Clontech), as packaging cells, were used according to the manufacturer's protocol. AmphiPack-293 cells were transfected with p45NF-E2 expression vector or empty vector. After 48 hours of transfection, retroviral supernatants were collected. OP9 cells were infected with the p45NF-E2 expression vector or empty vector (p45NF-E2-

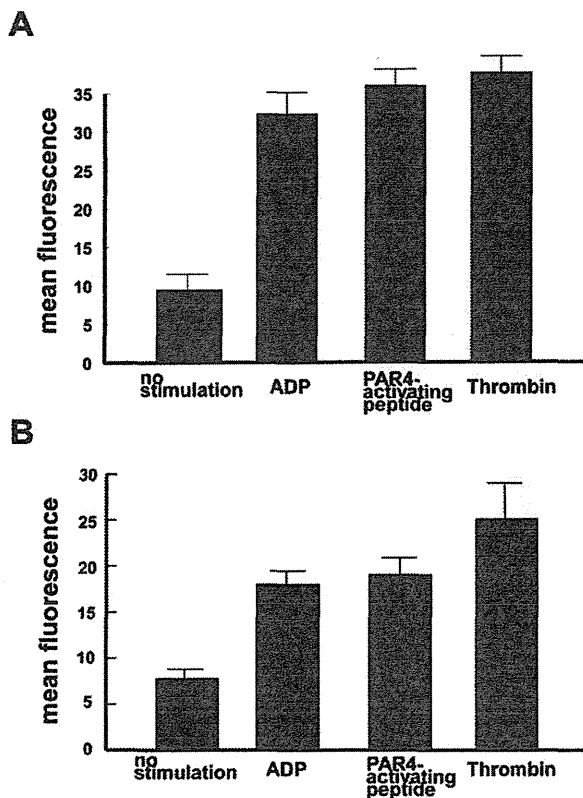


Figure 4. Functional analyses for OP9-derived platelets. **A**, By flowcytometry analysis, Alexa Fluor 488-labeled fibrinogen (100 μ g/ml) binding to platelets derived from OP9 cells was examined in the presence or absence of platelet stimulation reagents. **B**, The surface exposure of P-selectin was analyzed in the presence or absence of platelet stimulation reagents.
doi:10.1371/journal.pone.0058123.g004

OP9 and empty-OP9). Each of cells was cultured in MKLI medium for 12 days.

Statistics

Mean values of two groups were compared using Student's *t*-test. Statistical analysis was performed using StatView (ver 5.0, for Macintosh, SAS Institute Inc., Cary, NC). A *p* value of less than 0.05 was considered statistically significant.

Results

Differentiation of OP9 Cells into MKs and Platelets

We examined whether OP9 cells differentiate into MKs and platelets by using MKLI medium previously established to generate MKs and platelets from HSCs, ES cells, and pre-adipocytes. OP9 cells cultured for 6 days in MKLI medium resulted in adherent cells and a few floating cells. The OP9-derived cells on day 8 had adherent, loosely adherent, and floating cells, and most of cells on day 12 had floating cells (Figure S2A). Among OP9-derived cells on day 8, floating and loosely adherent cells morphologically resembling MKs derived from mBMMNCs cultured in MKLI medium (Figure S2B). These OP9-derived cells were characterized using surface markers, DNA polyploidy with nuclear staining, morphology using electron microscopy, and immunohistochemistry.

By flow cytometric analysis with MK lineage specific markers, approximately 95% and 60% of these OP9-derived MK-sized cells on day 8 expressed CD41, a surface marker throughout MK differentiation, and CD42b, a surface marker for the late stage of MK differentiation, respectively (Figure 1A). Approximately 70% and 60% of OP9-derived platelet-sized cells on day 12 expressed CD41 and CD42b, respectively (Figure 1B). Regarding the number of the OP9-derived MKs and platelets, approximately 4×10^4 MKs and 1×10^5 platelets were generated from 1×10^6 OP9 cells before the MK induction. OP9 cells before the MK induction (day 0) did not express CD41 and CD42b (Figure 1A, 1B). DNA ploidy of OP9-derived CD41+ cells ranged from 2N to 32N (Figure 1C). Immunohistochemical analyses showed that VWF and P-selectin, cytoplasmic proteins of MK lineage cells, were positive in OP9-derived CD41+ cells (Figure 2A, 2B). Under electron microscopic observation, OP9-derived MK-sized CD41+ cells had typical organelles for MKs, such as granules, demarcation membrane system, and lobulated nuclei, and OP9-derived platelet-sized CD41+ cells showed typical features for platelets, such as granules, mitochondria, and open canalicular system (Figure 2C, 2D). The present observations were similar to what described in MKs derived from mBMMNCs (Figure S3). Also, the present observations were similar to what described in MKs and platelets derived from mouse ES cells, mouse pre-adipocyte cell line 3T3-L1, human bone marrow CD34-positive cells, and human adipose tissues [19,20]. OP9-derived MK-sized CD41+ cells were examined for proplatelet formation under scanning electron microscopic observation. We observed proplatelets forming OP9-derived MK-sized CD41+ cells (Figure 3A). Moreover, proplatelet-forming OP9-derived MK showing CD41 and alpha-tubulin was observed (Figure 3B). To examine whether OP9-derived platelets are functional, fibrinogen-binding assay was performed on OP9-derived platelet-sized cells on day 12. Binding of Alexa Fluor 488-labeled fibrinogen to OP9-derived platelet-sized cells was increased upon stimulation when assessed by mean fluorescence (mean \pm S.D.): 9.7 ± 0.9 (no stimulation), 25.7 ± 0.3 (10 μ M ADP), $p < 0.0001$ (vs no stimulation), 28.6 ± 0.4 (1.5 mM PAR4-activating peptide), $p < 0.0001$ (vs no stimulation), and 29.2 ± 1.6 (0.5 U/ml thrombin), $p < 0.0001$ (vs no stimulation) (Figure 4A). The representative data of dot-plots in this assay are shown in Figure S4. Moreover, P-selectin surface exposure, a marker for platelet activation, on OP9-derived platelet-sized cells on day 12 was examined in the presence or absence of stimulation, and mean fluorescence (mean \pm S.D.) was 7.8 ± 1.1 (no stimulation), 17.9 ± 1.5 (10 μ M ADP), $p = 0.0159$ (vs no stimulation), 19.1 ± 1.8 (1.5 mM PAR4-activating peptide), $p = 0.0162$ (vs no stimulation), and 25.1 ± 3.8 (0.5 U/ml thrombin), $p = 0.0162$ (vs no stimulation) (Figure 4B). These observations indicated that OP9 cells differentiated into MKs and platelets *in vitro*.

Analyses of Gene Expressions of OP9 Cells during MK Differentiation

We then analyzed gene expression of candidate factors to elucidate mechanisms for the differentiation of OP9 cells into MKs and platelets. To examine whether this conversion goes through the status of cell pluripotency, the expressions of OCT3/4, specifically expressed in pluripotent cells, and SOX2, a key factor for the maintenance of cell pluripotency [34,35], were analyzed. Expression of both OCT3/4 and SOX2 was not detected in OP9 cells (day 0) and OP9-derived cells by RT-PCR (Figure 5). We also analyzed the gene expressions for transcription factors, p45NF-E2, FOG, Fli1, GATA1, GATA2, and RUNX1, that regulate megakaryopoiesis and thrombopoiesis [5–11]. These transcription factors, except for GATA1, were clearly detected in OP9 (day 0)

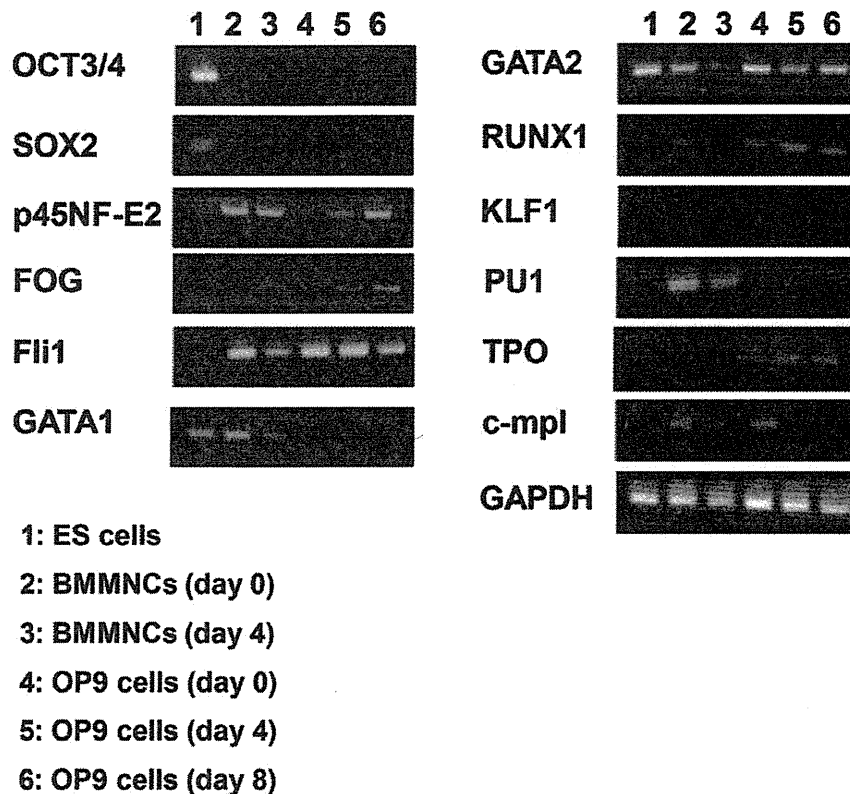


Figure 5. Analyses of gene expression of OP9 cells during megakaryocyte differentiation. Gene expression assessed by reverse transcription-PCR.
 doi:10.1371/journal.pone.0058123.g005

and OP9-derived cells (days 4 and 8) (Figure 5). Because major cell population of BMMNCs on day 4 morphologically resembled that of OP9-derived cells on day 8, we used BMMNCs on days 0 and 4 as a control. OP9 cells (day 0) also showed gene expression of TPO and *c-mpl*, receptor for TPO (Figure 5). Regarding the key transcription factors for other hematopoietic cell lineages, PU.1 for leukocytes [36] and KLF1 for erythrocytes [37], were not detected in OP9 cells (day 0) and OP9-derived cells (days 4 and 8) (Figure 5). Among the observed transcription factors, p45NF-E2 expression was increased during the differentiation of OP9 cells into MKs, and expression levels of p45NF-E2 in OP9 cells (day 0) and OP9-derived cells (day 4) were measured by quantitative real-time PCR analysis. It was found that expression levels of OP9-derived cells (day 4) had 3.91 ± 0.08 -fold higher than that of OP9 cells (day 0). Other transcription factors were also measured. It was for 1.54 ± 0.02 -fold higher for FOG, 0.03 ± 0.00 (0.0007)-fold higher for Fli1, 0.20 ± 0.03 -fold higher for GATA2, and 1.00 ± 0.16 -fold higher for RUNX1, as compared with those of OP9 cells (day 0). TPO expression levels of OP9-derived cells (day 4) had 3.59 ± 0.70 -fold higher than that of OP9 cells (day 0). *c-mpl* expression levels of OP9-derived cells (day 4) had 0.182 ± 0.11 -fold higher than that of OP9 cells (day 0). These results indicate that OP9 cells possess critical factors for MK differentiation and platelet production. Among them, the p45NF-E2 expression was increased during the differentiation of OP9 cells into MK lineages.

Enhanced Production of MKs and Platelets from OP9 cells Transfected with p45NF-E2

Based on increased expression of p45NF-E2 during differentiation of OP9 cells into MK lineages, we further studied the effect of OP9 cells transfected with p45NF-E2 on MK and platelet production. Transfection efficiency was estimated by DsRed expression, and approximately 50% of transfected OP9 cells was positive for DsRed expression, as assessed by flowcytometry (data not shown). Gene expression levels, assessed by qRT-PCR, of p45NF-E2 in p45NF-E2-OP9 cells on day 4 had 37.68 ± 11.36 -fold higher than that in empty-vector-OP9 cells. The p45NF-E2-OP9 cells and empty-vector-OP9 cells were cultured in MKLI medium for 12 days. By flow cytometric analysis, nearly all of the p45NF-E2-OP9-derived MK-sized cells on day 7 expressed CD41, whereas approximately 60% of empty-vector-OP9-derived MK-sized cells on day 7 expressed CD41 (Figure 6A). Also, CD42b expression was approximately 50% and 20% of p45NF-E2-OP9- and empty-vector-OP9-derived MK-sized cells on day 7, respectively (Figure 6A). The 1×10^6 OP9 cells (day 0) generated $3.3 \pm 1.8 \times 10^4$ MKs for p45NF-E2-OP9 cells and $2.2 \pm 1.6 \times 10^4$ ($p = 0.4008$) MKs for empty-vector-OP9 cells. The effect of p45NF-E2-overexpressing OP9 cells on platelet production was also examined. CD41 expression was approximately 50% and 20% of p45NF-E2-OP9- and empty-vector-OP9-derived platelet-sized cells on day 12, respectively (Figure 6B), and CD42b expression was approximately 20% and 10% of p45NF-E2-OP9- and empty-vector-OP9-derived platelet-sized cells on day 12, respectively (Figure 6B). It was found that the number of p45NF-

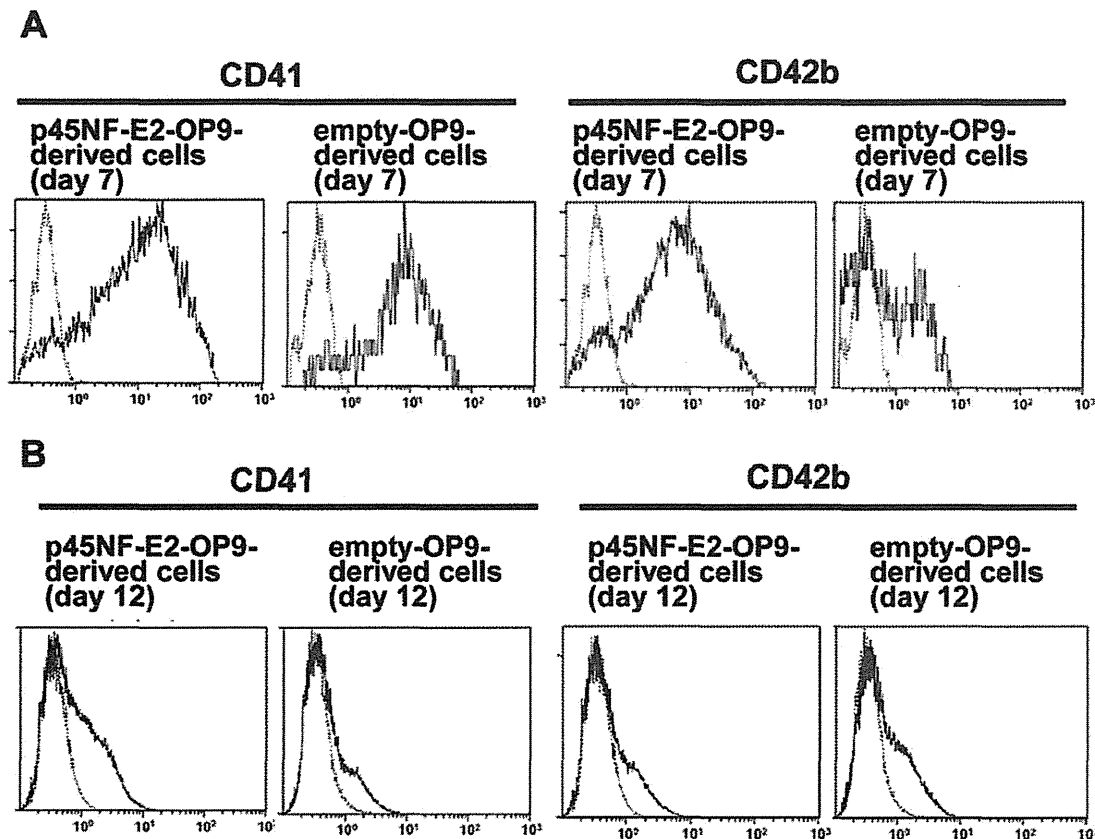


Figure 6. Production of megakaryocytes and platelets from OP9 cells transfected with p45NF-E2. **A**, Representative flowcytometry histogram of CD41 and CD42b expression on megakaryocyte-sized cells in each of samples introduced with the indicated vectors. Dot-line shows data using isotype control. **B**, Representative flowcytometry histogram of CD41 and CD42b expression on platelet-sized cells in each of samples introduced with the indicated vectors. Dot-line shows data using isotype control. doi:10.1371/journal.pone.0058123.g006

E2-OP9-derived platelet-sized CD41+ cells on day 12 showed approximately 3-fold higher than those in the empty-vector-OP9-derived platelet-sized CD41+ cells on day 12. The number of platelets generated from 1×10^6 OP9 cells (day 0) was $2.9 \pm 2.6 \times 10^5$ for the p45NF-E2-OP9-derived platelets and $1.0 \pm 7.3 \times 10^5$ ($p = 0.0518$) for the empty-vector-OP9-derived platelets. These findings indicate that p45NF-E2 has a critical role in the generation of MKs and platelets from OP9 cells, although the production of MKs and platelets was not significantly different between the p45NF-E2-OP9 cells and empty-vector-OP9 cells.

Discussion

This study demonstrated that OP9 cells differentiated into MKs and platelets *in vitro* using MKLI medium previously established to differentiate HSC, ES cells, pre-adipocytes into MK lineages. The present findings provide the first evidence for the differentiation of OP9 cells into MK lineages. Regarding the efficiency of the MK and platelet production from OP9 cells, approximately 4×10^4 MKs and 1×10^5 platelets were generated from 1×10^6 OP9 cells. On the other hand, 1×10^6 human bone marrow mononuclear cells produced approximately 6×10^3 MKs and 3×10^3 platelets in a similar culture scale using MKLI medium [24]. Although it is difficult to compare precisely the efficiency of

the MK and platelet production among various stem cell sources, our observations suggested that OP9 cells possess high capacity of the differentiation into MK lineages *in vitro*.

OP9 cells cultured in maintenance medium express specific surface marker for MSC and were reported to be pre-adipocytes [28,29]. These cell lineage fate of mesenchymal cells is distinct from that of HSCs, and OP9 cells are widely used as feeder cells for differentiation of iPS cells and ES cells into hematopoietic cells and MK lineages [12–15,25–27]. However, the present study shows that OP9 cells themselves are the source of MKs and platelets. OP9-derived MKs and platelets were characterized by specific surface markers, DNA polyploidy, morphology using electron microscopy, and immunohistochemistry. These analyses have been performed on *in vitro*-generated MKs and platelets beginning with cell sources including HSCs, ES cells, and iPS cells. When MKs and platelets derived from iPS cells or ES cells are harvested in the differentiation study using OP9 co-culture system, there is a possibility that some of MK lineage cells are derived from OP9 cells.

The gene expression analyses indicated that differentiation of OP9 cells into MK lineages did not share the common mechanism with pluripotent cells. OP9 cells possess the important factors related to megakaryopoiesis and thrombopoiesis, and these observations are compatible with our previous findings that 3T3-L1 pre-adipocytes possess GATA2, RUNX1, Fli1, FOG1, and

p45NF-E2. The expression of GATA1 was not detected in OP9 cells and 3T3-L1 cells [19]. Furthermore, we did not observe the GATA1 expression during differentiation of OP9 cells into MKs. Although GATA1 was reported to be a critical factor for the erythroid and MK development, previous studies demonstrated that GATA2 coordinates MK differentiation in GATA1 deficient and mutant cells [38]. Also, the present study revealed that the differentiation of OP9 cells into MK lineages involves in a p45NF-E2-mediated mechanism. The NF-E2 transcriptional factor is a basic-leucine zipper hetero-dimer complex consisting of p45 subunit, known as tissue-restricted subunit, and the small Maf proteins, Maf K and Maf G, known as widely expressed in many cells [39–45]. Observations in p45NF-E2 deficient MKs suggested that p45NF-E2 is important in the MK terminal differentiation and platelet release [46,47]. On the other hand, the *in vitro* and *in vivo* study using p45NF-E2-overexpressing bone marrow cells showed additional roles of p45NF-E2 in early megakaryopoiesis [48]. We previously reported that fibroblasts transfected with p45NF-E2, Maf G and Maf K differentiated into MKs and platelets, whereas fibroblast did not differentiate into MK lineage cells. These observations support p45NF-E2, Maf G, and Maf K as critical factors for megakaryopoiesis and thrombopoiesis. In the present study, OP9 cells have Maf G and Maf K, and thus cells were transfected with P45NF-E2. The present findings provide additional information for the importance of p45NF-E2 in megakaryopoiesis and thrombopoiesis. Further studies are definitely needed to elucidate the detailed pathways that cause OP9 cells to differentiate into the MK lineage ultimately leading to platelet production.

In summary, OP9 cells differentiated into MKs and platelets, although OP9 cells have been widely used as feeder cells in differentiation of ES cells and iPS cells into MKs and platelets. OP9 cells possess critical factors related to megakaryopoiesis and thrombopoiesis. The generation of MKs and platelets from OP9

cells could have important implications for study on the underlying mechanisms of megakaryopoiesis and thrombopoiesis.

Supporting Information

Figure S1 The plot of mouse platelets in flow cytometric analysis.

(TIFF)

Figure S2 Megakaryocyte lineage cells were generated from OP9 cells in vitro. A, Schematic outline and pictures for OP9 cells and differentiated stages into megakaryocyte lineages. B,

Mouse bone marrow mononuclear cells were cultured in megakaryocyte lineage induction media for 7 days.

(TIFF)

Figure S3 Transmission electron micrograph of mouse bone marrow mononuclear cells.

(TIFF)

Figure S4 Alexa Fluor 488-labeled fibrinogen binding to platelets derived from OP9 cells was examined in the presence or absence of platelet stimulation reagents.

(TIFF)

Acknowledgments

The authors thank Ms. Atsuko Igari and Ms. Yoko Sakanoue for technical assistance.

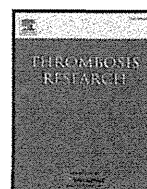
Author Contributions

Conceived and designed the experiments: YM YI. Performed the experiments: YM YO HS. Analyzed the data: FA TS MM. Contributed reagents/materials/analysis tools: YM HS MM YI. Wrote the paper: YM YO YI.

References

- Rao AK. (2003) Inherited defects in platelet signaling mechanisms. *J Thromb Haemost* 1: 671–681.
- Davi G, Patrono C. (2007) Platelet activation and atherothrombosis. *N Engl J Med* 357: 2482–2494.
- Clemetson KJ. (2012) Platelets and primary haemostasis. *Thromb Res* 129: 220–224.
- Kuter DJ. (1996) The physiology of platelet production. *Stem Cells* 14: 88–101.
- Pang L, Weiss MJ, Poncz M. (2005) Megakaryocyte biology and related disorders. *J Clin Invest* 115: 3332–3338.
- Deutsch VR, Tomer A. (2006) Megakaryocyte development and platelet production. *Br J Haematol* 134: 453–466.
- Chang Y, Bluteau D, Debili N, Vainchenker W. (2007) From hematopoietic stem cells to platelets. *J Thromb Haemost* 5: 318–327.
- Battinelli EM, Hartwig JH, Italiano JE. (2007) Delivering new insight into biology of megakaryopoiesis and thrombopoiesis. *Curr Opin Hematol* 14: 419–426.
- Kaushansky K. (2008) Historical review: megakaryocytopoiesis and thrombopoiesis. *Blood* 111: 981–986.
- Geddis AE. (2010) Megakaryopoiesis. *Semin Hematol* 47: 212–219.
- Reems JA, Pineault N, Sun S. (2010) In vitro megakaryocyte production and platelet biogenesis: state of the art. *Transfus Med Rev* 24: 33–43.
- Eto K, Murphy R, Kerrigan SW, Bertoni A, Stuhlmann H, et al. (2002) Megakaryocytes derived from embryonic stem cells implicate Ca_v1DAG-GEF1 integrin signaling. *Proc Natl Acad Sci USA* 99: 12819–12824.
- Fujimoto TT, Kohata S, Suzuki H, Miyazaki H, Fujimura K. (2003) Production of functional platelets by differentiated embryonic stem (ES) cells in vitro. *Blood* 102: 4044–4051.
- Gaur M, Kamata T, Wang S, Moran B, Shattil SJ, et al. (2006) Megakaryocytes derived from human embryonic stem cells: a genetically tractable system to study megakaryocytopoiesis and integrin function. *J Thromb Haemost* 4: 436–442.
- Takayama N, Nishikii H, Usui J, Tsukui H, Sawaguchi A, et al. (2008) Generation of functional platelets from human embryonic stem cells in vitro via ES-sacs, VEGF-promoted structures that concentrate hematopoietic progenitors. *Blood* 111: 5298–5306.
- Nishikii H, Eto K, Tamura N, Hattori K, Heissig B, et al. (2008) Metalloproteinase regulation improves in vitro generation of efficacious platelets from mouse embryonic stem cells. *J Exp Med* 205: 1917–1927.
- Fuentes R, Wang Y, Hirsch J, Wang C, Rauova L, et al. (2010) Infusion of mature megakaryocytes into mice yields functional platelets. *J Clin Invest* 120: 3917–3922.
- Takayama N, Nishimura S, Nakamura S, Shimizu T, Ohnishi R, et al. (2010) Transient activation of c-MYC expression is critical for efficient platelet generation from human induced pluripotent stem cells. *J Exp Med* 207: 2817–2830.
- Ono Y, Wang Y, Suzuki H, Okamoto S, Ikeda Y, et al. (2012) Induction of functional platelets from mouse and human fibroblasts by p45NF-E2/Maf. *Blood* 120: 3812–3821.
- Matsubara Y, Saito E, Suzuki H, Watanabe N, Murata M, et al. (2009) Generation of megakaryocytes and platelets from human subcutaneous adipose tissues. *Biochem Biophys Res Commun* 378: 716–720.
- Matsubara Y, Suzuki H, Ikeda Y, Murata M. (2010) Generation of megakaryocytes and platelets from preadipocyte cell line 3T3-L1, but not the parent cell line 3T3, *in vitro*. *Biochem Biophys Res Commun* 402: 796–800.
- Matsubara Y, Murata M, Ikeda Y. (2012) Culture of megakaryocytes and platelets from subcutaneous adipose tissue and a preadipocyte cell line. *Methods Mol Biol* 788: 249–258.
- Kerrigan SW, Gaur M, Murphy RP, Shattil SJ, Leavitt AD. (2004) Caspase-12: a developmental link between G-protein-coupled receptors and integrin α IIb β 3 activation. *Blood* 104: 1327–1334.
- Ono M, Matsubara Y, Shibano T, Ikeda Y, et al. (2011) GSK-3 β negatively regulates megakaryocyte differentiation and platelet production from primary human bone marrow cells *in vitro*. *Platelets* 22: 196–203.
- Nakano T, Kodama H, Honjo T. (1994) Generation of lymphohematopoietic cells from embryonic stem cells in culture. *Science* 265: 1098–1101.
- Niwa A, Umeda K, Chang H, Saito M, Okita K, et al. (2009) Orderly hematopoietic development of induced pluripotent stem cells via Flk-1(+) hemoangiogenic progenitors. *J Cell Physiol* 221: 367–377.
- Kitajima K, Minehata K, Sakimura K, Nakano T, Hara T. (2011) In vitro generation of HSC-like cells from murine ESCs/iPSCs by enforced expression of LIM-homeobox transcription factor Lhx2. *Blood* 117: 3748–3758.

28. Gao J, Yan XL, Li R, Liu Y, He W, et al. (2010) Characterization of OP9 as authentic mesenchymal stem cell line. *J Genet Genomics* 37: 475–482.
29. Wolins NE, Quaynor BK, Skinner JR, Tzekov A, Park C, et al. (2006) OP9 mouse stromal cells rapidly differentiate into adipocytes: characterization of a useful new model of adipogenesis. *J Lipid Res* 47: 450–460.
30. Hooper M, Hardy K, Handyside A, Hunter S, Monk M (1987) HPRT-deficient (Lesch-Nyhan) mouse embryos derived from germline colonization by cultured cells. *Nature* 326: 292–295.
31. Masui S, Nakatani Y, Toyooka Y, Shimosato D, Yagi R, et al. (2007) Pluripotency governed by Sox2 via regulation of Oct3/4 expression in mouse embryonic stem cells. *Nat Cell Biol* 9: 625–635.
32. Suzuki H, Kaneko T, Sakamoto T, Nakagawa M, Miyamoto T, et al. (1994) Redistribution of alpha-granule membrane glycoprotein IIb/IIIa (integrin alpha IIb beta 3) to the surface membrane of human platelets during the release reaction. *J Electron Microscop* (Tokyo) 43: 282–289.
33. Suzuki H, Murasaki K, Kodama K, Takayama H. (2003) Intracellular localization of glycoprotein VI in human platelets and its surface expression upon activation. *Br J Haematol* 121: 904–912.
34. Lewitzky M, Yamanaka S. (2007) Reprogramming somatic cells towards pluripotency by defined factors. *Curr Opin Biotechnol* 18: 467–473.
35. Colman A, Dreesen O. (2009) Induced pluripotent stem cells and the stability of the differentiated state. *EMBO rep* 10: 714–721.
36. Gupta P, Gurudutta GU, Saluja D, Tripathi RP. (2009) PU.1 and Partners: Regulation of Hematopoietic Stem Cell Fate in Normal and Malignant Hematopoiesis. *J Cell Mol Med* 13: 4349–4363.
37. Bieker JJ. (2005) Probing the onset and regulation of erythroid cell-specific gene expression. *Mt Sinai J Med* 72: 333–338.
38. Vicente C, Conchillo A, Garcia-Sánchez MA, Odero MD. (2012) The role of the GATA2 transcription factor in normal and malignant hematopoiesis. *Crit Rev Oncol Hematol* 82: 1–17.
39. Mignotte V, Wall L, deBoer E, Grosveld F, Romeo PH. (1989) Two tissue-specific factors bind the erythroid promoter of the human porphobilinogen deaminase gene. *Nucleic Acids Res* 17: 37–54.
40. Ney PA, Andrews NC, Jane SM, Safer B, Purucker ME, et al. (1993) Purification of the human NF-E2 complex: cDNA cloning of the hematopoietic cell-specific subunit and evidence for an associated partner. *Mol Cell Biol* 13: 5604–5412.
41. Peters LL, Andrews NC, Eicher EM, Davidson MB, Orkin SH, et al. (1993) Mouse microcytic anaemia caused by a defect in the gene encoding the globin enhancer-binding protein NF-E2. *Nature* 362: 768–770.
42. Chan JY, HanX-L, Kan YW. (1993) Isolation of cDNA encoding the human NF-E2 protein. *Proc Nat Acad Sci* 90: 11366–11370.
43. Igarashi K, Kataoka K, Itoh K, Hayashi N, Nishizawa M, et al. (1994) Regulation of transcription by dimerization of erythroid factor NF-E2 p45 with small Maf proteins. *Nature* 367: 568–572.
44. Andrews NC, Erdjument-Bromage H, Davidson MB, Tempst P, Orkin SH. (1993) Erythroid transcription factor NF-E2 is a haematopoietic-specific basic-leucine zipper protein. *Nature* 362: 722–728.
45. Andrews NC. (1998) The NF-E2 transcription factor. *Int J Biochem Cell Biol* 30: 429–432.
46. Shivdasani RA, Rosenblatt MF, Zucker-Franklin D, Jackson CW, Hunt P, et al. (1995) Transcription factor NF-E2 is required for platelet formation independent of the actions of thrombopoietin/MGDF in megakaryocyte development. *Cell* 81: 695–704.
47. Shivdasani RA. (2001) Molecular and transcriptional regulation of megakaryocyte differentiation. *Stem Cells* 19: 397–407.
48. Fock EL, Yan F, Pan S, Chong BH. (2008) NF-E2-mediated enhancement of megakaryocytic differentiation and platelet production in vitro and in vivo. *Exp Hematol* 36: 78–92.



Regular Article

Studies of a microchip flow-chamber system to characterize whole blood thrombogenicity in healthy individuals

Yusuke Yamaguchi ^a, Takanori Moriki ^{b,*}, Atsuko Igari ^a, Yumiko Matsubara ^a, Tomoko Ohnishi ^c, Kazuya Hosokawa ^c, Mitsuru Murata ^a

^a Department of Laboratory Medicine, Keio University School of Medicine, Tokyo, Japan

^b Health Center, Keio University, Tokyo, Japan

^c Research Institute, Fujimori Kogyo Co., Yokohama, Kanagawa, Japan

ARTICLE INFO

Article history:

Received 29 November 2012

Received in revised form 20 April 2013

Accepted 27 May 2013

Available online 16 June 2013

Keywords:

Thrombus formation

Platelet

Flow-chamber system

Thrombogenicity

ABSTRACT

Introduction: A whole blood flow-chamber system, the Total Thrombus-formation Analysis System (T-TAS), was developed for quantitative analysis of platelet thrombus formation (PTF) using microchips with thrombogenic surfaces (collagen, PL chip; collagen plus tissue thromboplastin, AR chip) under shear stress conditions. We evaluated the usefulness of the T-TAS for assessing individual thrombogenicity compared with other platelet function tests.

Materials and Methods: Blood samples from 31 healthy volunteers were applied to the T-TAS to measure PTF starting time (T_{10} : time to reach 10 kPa), occlusion time (T_{60} for PL chip; T_{80} for AR chip), and area under the curve (AUC_{10} , area under curve until 10 min for PL chip; AUC_{30} , 30 min for AR chip) under various shear rates (1000, 1500, 2000 s^{-1} for PL chip; 300 s^{-1} for AR chip). Platelet functions were also tested using platelet aggregometry, the PFA-100 (collagen and epinephrine [C/EPI], collagen and adenosine diphosphate [C/ADP]), and the VerifyNow P2Y12 assay.

Results: Individual pressure waveforms, including PTF starting and ending points, varied among healthy subjects. In the PL chip, T_{10} and AUC_{10} showed a shear-dependent correlation with C/EPI or C/ADP. VerifyNow P2Y12 values were not significantly associated with the parameters of the T-TAS. Platelet counts were correlated with all AR measurements, and mostly with PL measurements.

Conclusion: The results of the T-TAS were associated with those of the PFA-100 in many respects, indicating that its characteristics are related to shear-induced PTF. The T-TAS showed few correlations with platelet aggregometry and the VerifyNow P2Y12 assay. The T-TAS may allow for the measurement of comprehensive parameters of individual thrombogenicity under whole blood flow conditions.

© 2013 Elsevier Ltd. All rights reserved.

Introduction

The initial step of thrombus formation at the site of vascular injury in an artery is the adhesion of platelets to the exposed collagen-bound von Willebrand Factor (VWF), followed by platelet activation to bind stably to the collagen on the subendothelium under high-shear blood flow. Activated platelets undergo morphologic changes and aggregate together by bridging with VWF and fibrinogen, and release soluble agonists such as adenosine diphosphate, thromboxane A_2 , and thrombin, which further enhance platelet activation. The coagulation pathway on the platelet plasma membrane is accelerated to generate localized thrombin, leading to enhanced platelet activation and fibrin formation, and resulting in the growth of platelet thrombus formation (PTF) [1,2].

This process, hemostasis, is essential for maintaining blood circulation *in vivo* to prevent blood loss due to bleeding.

Arterial thrombosis, however, is attributed to pathologic PTF at sites of atherosclerotic plaque rupture, which leads to ischemia or necrosis of the organs downstream, such as acute coronary syndrome, myocardial infarction, and ischemic stroke [3,4]. Arterial thrombotic diseases are a major cause of morbidity and mortality, particularly in industrialized countries, and the numbers continue to grow worldwide, increasing healthcare costs. Prothrombotic conditions, e.g., high platelet reactivity, enhanced coagulation, and reduced fibrinolysis, have been identified in disorders that lead to atherosclerotic thrombosis [5], such as diabetes [6,7], hypertension [8], dyslipidemia [9], obesity [10], and metabolic syndrome [11,12], as well as in smokers [13] and the elderly [14].

Evaluation of the prothrombotic status is expected to contribute to the primary prevention of arterial thrombosis by improving lifestyle habits, such as diet and exercise, or the consideration of antithrombotic medication, but the most appropriate test for evaluating thrombogenicity in an

* Corresponding author at: Health Center, Keio University, 35 Shinanomachi, Shinjuku-ku, Tokyo 160-8582, Japan. Tel.: +81 3 5363 3973; fax: +81 3 3359 6963.

E-mail address: TakaMoriki@aol.com (T. Moriki).